



UNIVERSITY OF CRETE
DEPARTMENT OF LIFE SCIENCES
FACULTY OF BIOLOGY

Post-graduate Studies Program
«Molecular Biology - Biomedicine»

DIPLOMA THESIS

“In vivo distribution of Mena in postnatal CNS synapses”

Supervisor: Dr. Marina Vidaki, PhD

Linardou Niki

Heraklion, September 2022

Examination Committee

❖ Dr. Marina Vidaki

Assistant Professor of Cellular-Molecular Biology, Faculty of Medicine,
Division of Basic Sciences, University of Crete

❖ Dr. Domna Karagogeos

Professor of Molecular Biology-Developmental Neurobiology, Faculty of
Medicine, Division of Basic Sciences, University of Crete

❖ Dr. Kyriaki Sidiropoulou

Assistant Professor of Neurophysiology, Department of Biology,
Neurophysiology and Behaviour Laboratory at University of Crete and
IMBB-FORTH

Summary

Neuronal networks constitute perhaps the most complex and intricate formations of an organism. Due to their oftentimes extensive dimensions, cellular compartments such as axons, dendrites, and synapses can be located at a considerable distance from the cellular body. However, they still contain the vast majority of the cytoplasm, and are responsible for many diverse functions. In order to maintain their neuronal homeostasis, the ability to respond rapidly to intra- and extra-cellular stimuli must be independently preserved for different sub-neuronal compartments.

Localized mRNA transport and translation are some of the mechanisms that allow for this spatiotemporal regulation. Although the exact molecular mechanism of local mRNA translation remains elusive, it appears to be based on the semi-autonomous protein translation of mRNA that has been specifically transported and stored in sub-neuronal compartments, in response to internal and external stimuli. Ribonucleoprotein complexes (RNPs) formed by RNA-binding Proteins (RBPs), mRNA molecules, and other regulatory proteins, play a crucial role in the transportation, as well as the regulation of the localized translation of these mRNA molecules. Local mRNA transportation and subsequent translation, along with the regulation of actin cytoskeleton, has been shown to have a key role in axon elongation and guidance, synaptogenesis, and post-development synaptic plasticity, among other processes. Its importance during neuronal development is highlighted by the fact that dysregulation of these two processes has been implicated in several neurodegenerative and neurodevelopmental disorders such as autism spectrum disorders (ASDs), Fragile X syndrome, spinal muscular atrophy (SMA) and amyotrophic lateral sclerosis (ALS).

Mena (ENAH) is a protein of the Ena/Vasp protein family and is highly expressed in the nervous system. Previous work from our lab has shown that, in addition to its role in actin cytoskeleton regulation Mena also plays a regulatory role in local translation; Mena has been found to form an RNP complex with known translation regulators HnrnpK and PCBP1 and cytosolic mRNAs in developing axons. The presence of Mena is required for translation of the associated mRNAs locally. This newly discovered dual nature of Mena's function raises several questions: does its general role in axonal local translation extend to other sub-cellular compartments, namely in synapses? Does it still interact with the same regulators, and if not, what other proteins does it interact with? The further elucidation of Mena's role could help us shed light on different neurodevelopmental disorders.

Mena's diverse role in the sub-cellular compartments of the NS remains for the greater part elusive, and so, in order to learn more about it, our lab has started a study on its spatiotemporal expression pattern throughout the developing mouse CNS. This project has brought this effort a step further, adding two new timepoints (P8-10 and P15 mice) to the preexisting ones (P22 and 2m.o. mice). We have continued to study Mena's localization across the entire CNS, using different neuronal and synaptic markers, and comparing our findings with the timepoints that were previously studied. We

discovered interesting similarities and differences across the different CNS structures and timepoints, and most importantly were able to acquire strong evidence of the synaptic localization of Mena in structures such as layers L2/3 and L5 of the Cortex, the Hippocampus, the Cerebellum, the Medulla, the Hindbrain, and the DRGs.

Furthermore, by testing and using a synaptoneurosome isolation method, followed by co-immunoprecipitation, we were able to test Mena's interaction in synapses with several molecules of interest: EVL, VASP, EEF2, SAFB, HNRNPK, and PCBP1. Mena was found to interact with EVL, VASP, EEF2, and SAFB but, surprisingly, no interaction was observed for known developmental interactors HNRNPK and PCBP1. This presents a very interesting avenue for future study and leads us to believe that Mena's interaction profile in the synapses could be quite different from its general neuronal one.

Keywords: local mRNA translation, actin cytoskeleton dynamics, synapses, synaptoneurosome isolation, immunohistochemistry, co-immunoprecipitation, Mena (ENAH), EVL, VASP, EEF2, SAFB, HNRNPK, PCBP1.

Περίληψη

Τα νευρωνικά δίκτυα αποτελούν ίσως τους πιο πολύπλοκους και περίπλοκους σχηματισμούς ενός οργανισμού. Λόγω των συχνά εκτεταμένων διαστάσεών τους, κυτταρικά διαμερίσματα όπως οι άξονες, οι δενδρίτες και οι συνάψεις είναι πιθανό να βρίσκονται σε σημαντική απόσταση από το κυτταρικό σώμα. Ωστόσο, τα συγκεκριμένα κυτταρικά διαμερίσματα εξακολουθούν να περιέχουν τη συντριπτική πλειονότητα του κυτταροπλάσματος και είναι υπεύθυνα για πολλές και ποικίλες λειτουργίες. Προκειμένου να διατηρήσουν τη νευρωνική ομοιόστασή τους, η ικανότητα ταχείας απόκρισης σε ενδοκυτταρικά και εξωκυτταρικά ερεθίσματα πρέπει να διατηρείται ανεξάρτητα για τα διάφορα νευρωνικά διαμερίσματα.

Η τοπική μεταφορά και η τοπική μετάφραση του mRNA είναι μερικοί από τους μηχανισμούς που επιτρέπουν αυτή τη χωροχρονική ρύθμιση. Αν και ο ακριβής μοριακός μηχανισμός της τοπικής μετάφρασης του mRNA παραμένει σε μεγάλο βαθμό άγνωστος, φαίνεται πως βασίζεται στην ημιαυτόνομη πρωτεϊνική μετάφραση του mRNA που έχει μεταφερθεί και αποθηκευτεί ειδικά σε υπονευρωνικά διαμερίσματα, σε απόκριση σε εσωτερικά και εξωτερικά ερεθίσματα. Τα ριβονουκλεοπρωτεϊνικά σύμπλοκα (RNPs) που σχηματίζονται από πρωτεΐνες που δεσμεύουν το RNA (RBPs), μόρια mRNA και άλλες ρυθμιστικές πρωτεΐνες, διαδραματίζουν κρίσιμο ρόλο στη μεταφορά, καθώς και στη ρύθμιση της τοπικής μετάφρασης αυτών των μορίων mRNA. Η τοπική μεταφορά mRNA και η επακόλουθη μετάφραση, μαζί με τη ρύθμιση του κυτταροσκελετού της ακτίνης, έχει αποδειχθεί ότι διαδραματίζουν βασικό ρόλο στην επιμήκυνση και καθοδήγηση των αξόνων, στη συναπτογένεση και στη συναπτική πλαστικότητα μετά την ανάπτυξη, μεταξύ άλλων διεργασιών. Η σημασία αυτών των δύο διεργασιών κατά τη διάρκεια της νευρωνικής ανάπτυξης αναδεικνύεται από το γεγονός ότι η απορρύθμιση τους έχει ενοχοποιηθεί για διάφορες νευροεκφυλιστικές και νευροαναπτυξιακές διαταραχές, όπως οι διαταραχές του φάσματος του αυτισμού (ASDs), το σύνδρομο Fragile X, η νωτιαία μυϊκή ατροφία (SMA) και η αμυοτροφική πλευρική σκλήρυνση (ALS).

Η Mena (ENAH) ανήκει στην πρωτεϊνική οικογένεια Ena/VASP και εκφράζεται σε μεγάλο βαθμό στο νευρικό σύστημα. Προηγούμενες μελέτες του εργαστηρίου μας έχουν δείξει πως η Mena διαδραματίζει επίσης ρυθμιστικό ρόλο στην τοπική μετάφραση. Έχει βρεθεί πως σχηματίζει ένα ριβονουκλεοπρωτεϊνικό σύμπλοκο με τους γνωστούς μεταφραστικούς ρυθμιστές HnnpK και PCBP1 καθώς και συγκεκριμένα μόρια mRNA στους αναπτυσσόμενους άξονες. Η παρουσία της Mena βρέθηκε ότι είναι απαραίτητη για τη μετάφραση των μεταγράφων αυτών τοπικά στους άξονες. Η πρόσφατα ανακαλυφθείσα διπλή φύση της Mena εγείρει διάφορα ερωτήματα: ο γενικός της ρόλος στην αξονική τοπική μετάφραση επεκτείνεται και σε άλλα υποκυτταρικά διαμερίσματα, και συγκεκριμένα στις συνάψεις; Εξακολουθεί να αλληλεπιδρά με τους ίδιους ρυθμιστές, και αν όχι, με ποιες άλλες πρωτεΐνες αλληλεπιδρά; Η περαιτέρω διαλεύκανση του ρόλου της Mena θα μπορούσε να μας βοηθήσει να κατανοήσουμε καλύτερα διάφορες νευροαναπτυξιακές διαταραχές.

Ο ποικίλος ρόλος της Mena στα υποκυτταρικά διαμερίσματα του ΝΣ παραμένει κατά το μεγαλύτερο μέρος ασύλληπτος, και έτσι, προκειμένου να μάθουμε περισσότερα γι' αυτόν, το εργαστήριό μας έχει ξεκινήσει να μελετάει το χωροχρονικό πρότυπο έκφρασής της σε όλο το αναπτυσσόμενο ΚΝΣ των ποντικών. Η παρούσα εργασία συνέχισε αυτή την προσπάθεια, προσθέτοντας δύο νέες χρονικές στιγμές μελέτης (ποντίκια P8-10 και P15) στις προϋπάρχουσες (ποντίκια P22 και 2m.o.). Συνεχίσαμε να μελετάμε τον εντοπισμό της Mena σε ολόκληρο το ΚΝΣ, χρησιμοποιώντας διαφορετικούς νευρωνικούς και συναπτικούς δείκτες, συγκρίνοντας τα ευρήματά μας με τα χρονικά σημεία που είχαν μελετηθεί προηγουμένως. Ανακαλύψαμε ενδιαφέρουσες ομοιότητες και διαφορές στις διάφορες δομές και χρονικές στιγμές του ΚΝΣ, και το πιο σημαντικό ήταν ότι μπορέσαμε να δούμε ισχυρές ενδείξεις για τον συναπτικό εντοπισμό της Mena σε δομές όπως οι στιβάδες L2/3 και L5 του φλοιού, ο ιππόκαμπος, η παρεγκεφαλίδα, ο προμήκης μυελός, ο οπίσθιος εγκέφαλος και τα σπονδυλικά νευρικά γάγγλια.

Επιπλέον, δοκιμάζοντας και χρησιμοποιώντας μια μέθοδο απομόνωσης συναπτοσωμάτων, ακολουθούμενη από πειράματα συνεργατικής ανοσοκατακρήμνισης, μπορέσαμε να ελέγξουμε την αλληλεπίδραση της Mena στις συνάψεις με διάφορα μόρια ενδιαφέροντος: EVL, VASP, EEF2, SAFB, HNRNPK και PCBP1. Διαπιστώθηκε ότι η Mena αλληλεπιδρά με τις πρωτεΐνες EVL, VASP, EEF2 και SAFB, αλλά, παραδόξως, δεν παρατηρήθηκε καμία αλληλεπίδραση για τους παράγοντες HNRNPK και PCBP1, οι οποίοι έχει βρεθεί πως αλληλεπιδρούν με την Mena σε προηγούμενες μελέτες. Αυτό παρουσιάζει μια πολύ ενδιαφέρουσα οδό μελλοντικής μελέτης και μας οδηγεί στην θεωρία ότι το προφίλ αλληλεπίδρασης της Mena στις συνάψεις είναι αρκετά διαφορετικό από αυτό στο γενικό νευρικό σύστημα.

Λέξεις-κλειδιά: τοπική μετάφραση mRNA, δυναμική του κυτταροσκελετού της ακτίνης, συνάψεις, απομόνωση συναπτοσωμάτων, ανοσοϊστοχημεία, συνεργατική ανοσοκατακρήμνιση, Mena (ENAH), EVL, VASP, EEF2, SAFB, HNRNPK, PCBP1.

Acknowledgments

The diploma thesis you are currently reading was completed in the Molecular and Cellular Neuroscience Lab of Dr. Marina Vidaki. I would like to thank her from the bottom of my heart for giving me the opportunity to work with her and her team. Words fall short to express my immense gratitude for her guidance, mentorship, and above all her genuine support. I am beyond honored to have been a member of her team. I would also like to express my gratitude to the two other members of my examination committee, Dr. Domna Karagogeos and Dr. Kyriaki Sidiropoulou. I have nothing but respect and admiration for their work, and am honored that they invested their time in mine.

Finally, to the lab members I had the opportunity to get to know and work with: First and foremost, to Manolis Agrymakis Ph.D., I owe more than a few thanks. His in-depth expertise and rigorous work set a high standard for my own continuation of his research project, one that I can only hope to match. With equal fervor, I would like to thank Elena Vorgia Ph.D., whose kindness, advice, and patient guidance were crucial during my acclimatization in the lab. I would also like to thank the other members of the lab: Nikoleta Triantopoulou Ph.D. for her empathy and wisdom, Sofia Pasadaki Ph.D. for her invaluable help and advice, and lastly Niki Throumpari BSc and Fotis Karitis BSc for their friendship and support.

Table of Contents

A – INTRODUCTION	10
A.1 RNA transport and local translation	11
A.2 Mena and its role in the NS	14
A.3 Project Outline.....	18
B - METHODS.....	20
B.1 Immunofluorescence	20
B.1.1 Cryosections.....	21
B.1.1.1 Perfusion.....	21
B.1.1.2 Encasement.....	21
B.1.1.3 Freezing.....	22
B.1.1.4 Cryosectioning.....	22
B.1.2 Immunohistochemistry.....	23
B.1.3 Imaging and Data Analysis.....	23
B.2 Synaptoneuroosomes.....	24
B.2.1 Synaptoneurosome Isolation.....	24
B.2.2 Co-Immunoprecipitation.....	25
B.2.3 Western Blot Analysis.....	26
C - RESULTS AND DISCUSSION.....	29
C.1 Immunofluorescence.....	29
C.1.1 Timepoint P8-10.....	29
C.1.2 Timepoint P15.....	37
C.2 Synaptoneuroosomes.....	42
C.3 Concluding remarks.....	44

D - SUPPLEMENTARY MATERIAL.....	46
Bibliography.....	46
Abbreviations.....	48
Table of IF experiments.....	49

A – INTRODUCTION

The nervous system is perhaps the most intriguing part of an organism, due to its intricate, complex, and diverse functionality. In order to perform their regulatory role in the body, as well as maintain neuronal homeostasis, neuronal components have oftentimes diverse and elaborate forms. A single neuron with its axon and numerous, expansive dendrites can reach impressive lengths (such as the sciatic nerve, whose axon often exceeds one meter in the human body). Despite their distance from the main body, axonal and dendritic compartments such as synaptic terminals and growth cones contain the majority of the cytoplasm (Biever et al., 2019) and are responsible for the constant exchange of information.

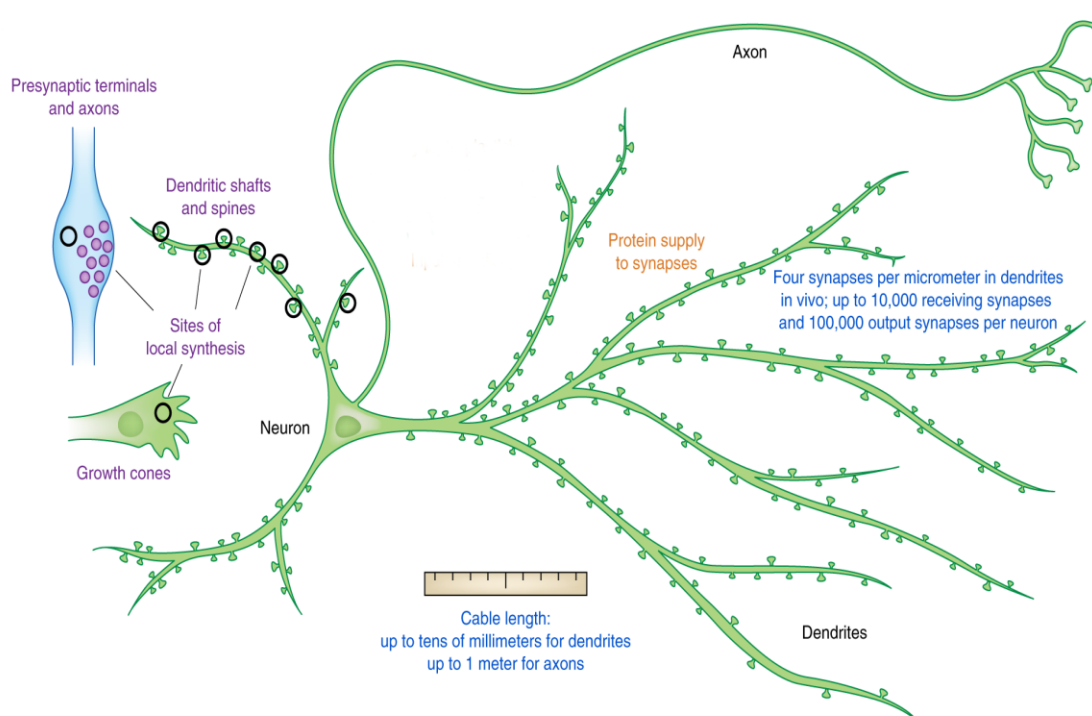


Image 1: A typical neuron and its compartments (modified from Holt et.al., 2019)

The synapses are a big part of our focus for this project; consisting of both pre- and post-synaptic compartments, their vast numbers (up to 10.000 receiving synapses and 100.000 output synapses per neuron, Holt et.al. 2019) allow for the formation of labyrinthine networks which weave the nervous system into existence. And although the main source of proteins, [involving important housekeeping proteins such as vesicular proteins and other transmembrane components like calcium channels and CAMS (Maas et.al., 2012)] to synapses is via cell body synthesis and subsequent translocation, mRNA localization and local translation (LT) plays an equally important role, being observed during development (growth cones) as well as in mature neurons (dendrites) (Kennedy et.al., 2006). LT is shown to be critical in axon guidance

(Vuppalanchi et.al., 2009). That is not surprising - the highly dynamic state of axons, which enables them to rapidly and effectively respond to stimuli, could not possibly be exclusively maintained by protein transportation from the neuron's main body. That is because of a series of challenges, namely the low propagation speed of cytoskeletal and cytosolic proteins (a few millimeters per day on average) compared to the oftentimes vast distances that need to be traversed, as well as the limited half-life of synaptic proteins (Giuditta et.al., 2002). Thus, the need for alternative mechanisms was raised, mechanisms that can account for the different sub-neuronal compartments' need for the decentralization of many of the processes imperative to a cell's function.

A.1 RNA Transport and local Translation

Two highly conserved mechanisms that have been developed for this purpose are targeted mRNA transport, or localization, and local mRNA translation (Cioni et al., 2018). In this manner, protein expression can be regulated in a semi-autonomous, spatiotemporal manner; at the arrival of a signal, stored mRNA transcripts can be translated as needed, allowing the neuron to maintain the key processes that characterize its function. The entire translational machinery as well as a specific set of transcripts has been observed in dendritic synapses (Sutton et.al., 2006). Incidentally, the proteins synthesized in dendrites appear to produce proteins with specialized synaptic functions instead of general housekeeping genes. Some of these proteins include key kinases (CaMKII α , PKM ζ), cytoskeletal proteins (Arc, MAP2) and neurotransmitter receptors of the AMPA (GluR1 and 2) and NMDA (NR1) families (Bramham and Wells, 2007, Andreassi and Riccio, 2009, Wang et al, 2010). Synapses have also been found to contain a different proteome than the main body, comprising of as many as 2.500 different proteins (Holt et.al., 2019).

This evidence suggests that local translation is most likely regulated in an activity-dependent manner, enabling each individual synapse's functional and morphological modification, thereby providing a mechanism for synaptic plasticity (Martin et.al., 2009). Further elucidation of the mechanisms behind these processes might very well answer fundamental queries about the nervous system, as well as provide a new basis for understanding and hopefully tackling multiple neurodevelopmental and neurodegenerative disorders.

The localization of mRNA is a crucial regulatory mechanism of gene expression in the synapses and other sub-neuronal compartments, for several reasons. First of all, the localization of the transcriptome instead of the proteome serves in the targeted synthesis in the appropriate intracellular compartment, rendering its expression in other parts, in which it might not be needed, obsolete. That allows for protection of the cell, in the case of proteins that might be harmful to other parts of it, for example MBP in oligodendrocytes (Martin and Ephrussi, 2009). Second, it allows for a very finetuned spatiotemporal resolution of gene expression, which in turn allows a synapse to alter its

morphology and function, in a manner that is semi-independent from the cell body. Finally, it aids cell economy, allowing a single transcript to be translated on-site several times, instead of requiring each protein to be transported from the cell body to each distinct synapse (St. Johnston et al., 2005).

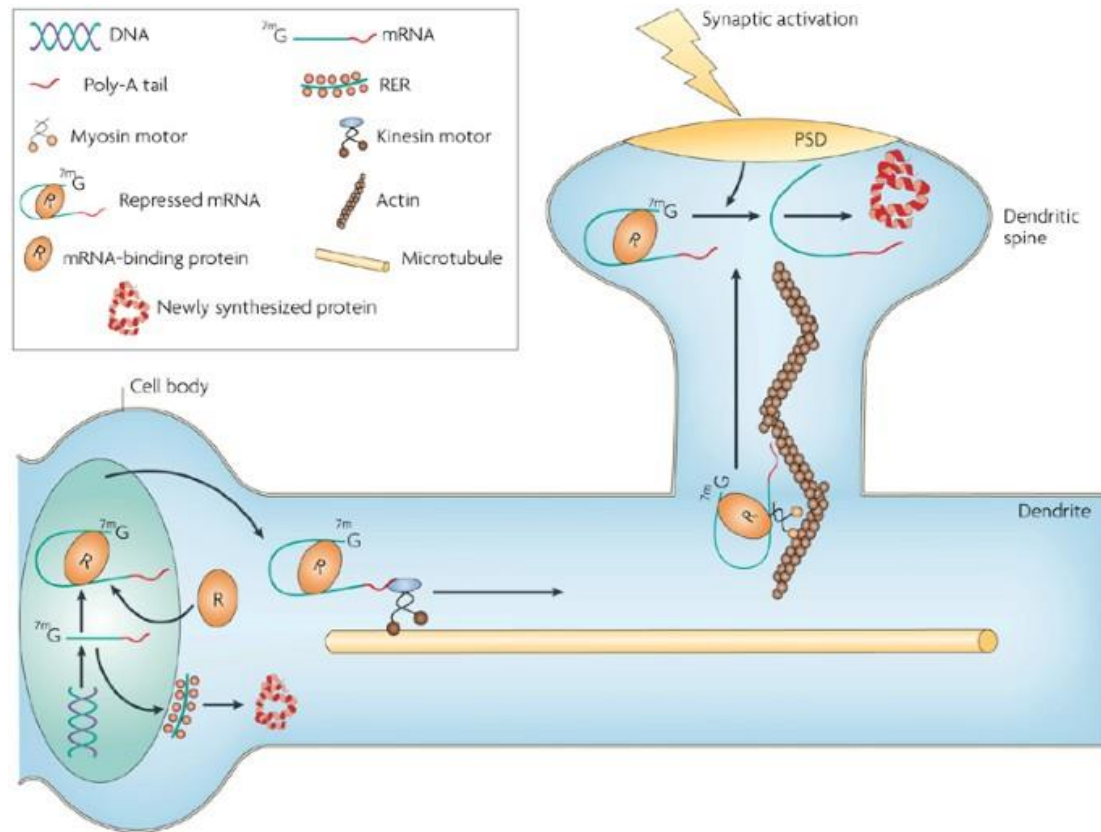


Image 2: Transport and translation of dendritic mRNA (Bramham et al., 2007).

The different parts of mRNA localization can be summed up in the following steps:

1. RBPs recognize signals in the 3'-untranslated region (3'-UTR) of transcripts.
2. RBPs create translationally repressed complexes with RNAs and RNPs.
3. Transport RNPs are translocated by motor-proteins towards their respective destinations along the microtubule cytoskeleton and subsequently anchored in the vicinity of activated synapses.
4. The localized mRNAs are translationally activated as needed (Doyle et al., 2011).

RNA-binding proteins (RBPs) are one of the largest categories of proteins in mammalian cells, with at least 380 neuronal RBPs encoded in the mouse genome. Several RBPs have been detected in axons, and are theorized to interact with many different mRNAs each, due to the comparatively large amount of mRNA that has been detected (Keene, 2007). Some RBPs form RNP (ribonucleoprotein) granules along with mRNA molecules, regulating the translation by either translational suppression (Kiebler et.al., 2006) or translational promotion (Ross et.al., 2014). Post-translational modifications of respective mRNA molecules allow for the rapid assembly and reassembly of RNA-RBP complexes. The translation of these mRNA molecules is usually suppressed while they remain in this complex, until the arrival of extracellular signals that promote local translation, allowing for the localized regulation at distal parts of the neuron such as synapses (Sasaki, 2020). Furthermore, actin cytoskeleton dynamics have also recently been correlated with local translation, on top of mRNA localization, due to proteins like APC which function as regulators of both microtubule dynamics and local protein synthesis (Cioni et.al., 2018), and mena that can regulate actin filament elongation and local translation (Vidaki et.al., 2017).

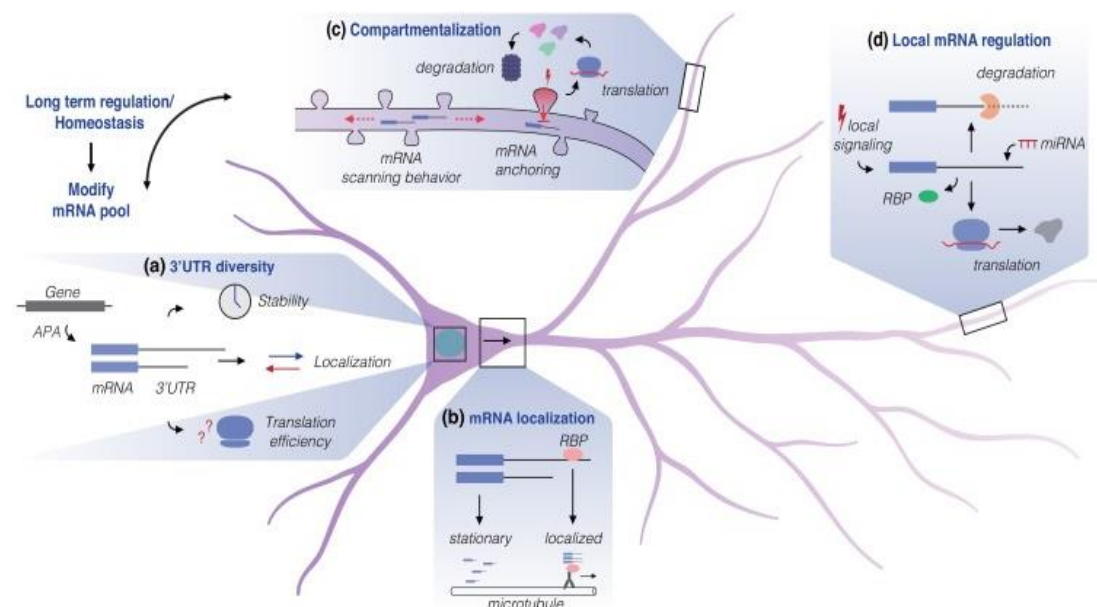


Image 3: Neuronal regulation of mRNA, Glock et.al., 2017

Following mRNA localization, local translation takes place in distal sites in a spatiotemporally regulated manner. Many recent studies are focusing on local translation, and much effort has been devoted to understanding the capacity and role of local protein synthesis in neuronal components. It has been shown that, especially during development, local translation plays a pivotal part in synaptogenesis, as its inhibition renders the presynaptic terminal unable to release neurotransmitter vesicles (Cioni et. al., 2018). Local translation is also integral in the correct function of growth

cones in the developing NS, enabling their high motility (Sasaki et.al., 2020) as well as in synapse strengthening, synapse elimination, and signal relay to the cell soma (Batista et.al., 2016). Local translation is not only involved in the development, as it has been shown to take part in an activity-dependent manner in mature neurons as well. Synaptic plasticity (Biever et.al., 2019) as well as long-term memory formation has been shown to be highly dependent on local translation (Cioni et.al., 2018).

The necessary components for this process are mRNA molecules, active ribosomes, and regulatory proteins such as RBPs. The localized mRNAs are of remarkable diversity, signifying the importance of local translation (Biever et.al., 2019). Although the presence of local mRNA translation has been proven for axons and their terminals for quite some time, recent studies have also placed it in dendrites and their post-synaptic compartments (Giuditta et.al., 2002). And although further research needs to be undertaken in the realm of pre-synaptic compartments, it has been heavily suggested that understanding the role of local protein synthesis in synaptic function will shed light on synaptic architecture and its activity-dependent modification.

With local transportation and translation taking part in so many integral cellular processes, it can come as no surprise how the disruption of any of these can have significant damaging results to the nervous system. Disrupted translation in growth cones and synapses has been involved in the pathophysiology of a number of neurodevelopmental and neurodegenerative disorders, resulting in intellectual disabilities or autism-related symptoms (Sasaki, 2020). Given that, according to the Centers for Disease Control and Prevention (CDC), an estimated 75 million people (1% of the entire world population) are characterized by an autism spectrum disorder (ASD), it is not hard to imagine the possible impact. ASDs have already been linked to a number of different gene mutations, and present a wide phenotypic heterogeneity (Akins et.al., 2009). Disruption in the function and structure of synapses has also been linked with other intellectual disabilities, such as schizophrenia, and fragile X syndrome (Kelleher et.al., 2008). The umbrella term for these intellectual disabilities is synaptopathies, as more than 50% of the genes related to them have been found to encode synaptic proteins. Fragile X syndrome and ASDs seem to have underlying local translation deficits (Bear et.al., 2008), leading researchers to believe that it might be a common feature with other similar disorders. Discrepancies in local translation have also been theorized to play a role in a number of degenerative disorders, for example spinal muscular atrophy (SMA), amyotrophic lateral sclerosis (ALS) (Liu-Yesucevitz et.al., 2011), Alzheimer's disease and Parkinson's disease (Lu et al., 2020). The multifaceted effects of dysregulated or disrupted local transportation and translation emphasize the significance of further research on their molecular mechanics.

A.2 Mena and its Role in the Nervous System

As previously mentioned, actin cytoskeleton dynamics have been correlated with local translation, due to proteins that function as regulators of both actin dynamics and local

protein synthesis. Mena is a protein with such function. Mena, an RNP-forming protein, controls local mRNA translation, while also playing a role in actin cytoskeleton remodeling, regulating synaptic function with its dual nature.

Mena, also known as ENAH, is the mammalian homolog of ENA (*Drosophila* Abl.). Its gene is located on chromosome 1, and it is expressed ubiquitously by many cell types and found in all tissue types, being at its most abundant in the NS. Out of the two known isoforms of Mena, one appears to be exclusively expressed in neurons. Its expression in tissues has been shown to decrease throughout maturation (Gurzu et.al., 2013). Along with its paralogs, VASP and EVL, they form a protein family most commonly located in areas with a need for dynamic actin remodeling, predominantly during the creation and expansion of filopodia and lamellipodia (Gupton et.al., 2007). They accomplish that via specific protein domains that allow for its direct interaction with actin's two forms: G-actin (or globular actin) and F-actin (or fibrous actin). In order to do that, the formation of tetramers consisting of Mena along with VASP and EVL is necessary. These tetramers also promote actin polymerization through Profilin1 (Gertler et.al., 2012).

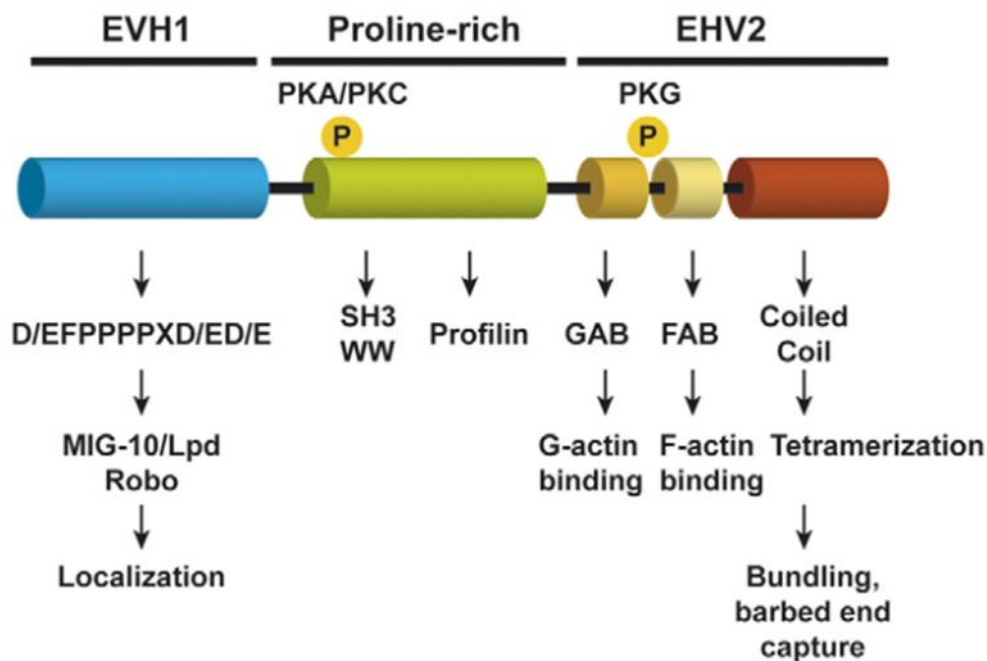


Image 4: Visual representation of the ENA family proteins' domains, Drees and Gertler, 2008

Although the ENA family protein domains are highly conserved (Image 4), Mena contains additional domains and sequences that are not found in either VASP or EVL (Gertler et.al., 2012). So far, a universal molecular mechanism for Mena's function as an actin regulator has not been found. However, because of its ability to control the dynamic movements of actin filaments, Mena has been strongly implicated in processes

that are based on this principle, such as phagocytosis, hemostasis, fibroblast movement, chemotaxis, migration and even metastasis. Mena and its various isoforms have, in recent years, been associated with a number of different cancer types, in particular in the process of metastasis. Mena's expression in cancerous tissues has been shown to increase, and its presence is therefore used as a molecular marker in forms of cancer such as breast, intestine, liver, pancreas, and cervix cancer (Gurzu et.al., 2013).

Mena, VASP and EVL are also required for normal development of the nervous system, and in particular in processes that require cell migration or cytoskeleton remodeling. Mena and its isoforms have been shown to be key regulators of overall NS development (Menzies et.al., 2004, Lanier et.al., 1999), neurogenesis, migration (Kwiatkowski et.al., 2007) dendritic morphology, synapse formation (Li et.al., 2005, Lin et.al., 2007), axon guidance and terminal axon branching (Dwivedy et.al., 2007). The proteins of the Ena family have also been shown to have a key role in the motility of growth cones; an artificial decrease in their levels in the growth cones promotes the creation of short and strongly branched actin filaments, while their overexpression promotes the creation of elongated, more far-reaching actin filaments (Menzies et.al., 2004). Mena deficiency has been shown to cause clear defects in NS development; Mena-deficient mice show malformation or no formation of the corpus callosum as well as misrouted spinal nerves (Menzies et.al., 2004).

Recently, Mena has been shown to have an additional role in the NS apart from actin regulation; according to Vidaki et.al. (2017), Mena has been found to be part of an mRNA regulon together with Safb2, and the RBPs HnRNPk and PCBP1. These proteins participate in the formation of an RNP complex along with cytosolic mRNAs, which then is transferred to developing axons and is translated in an activity-dependent manner.

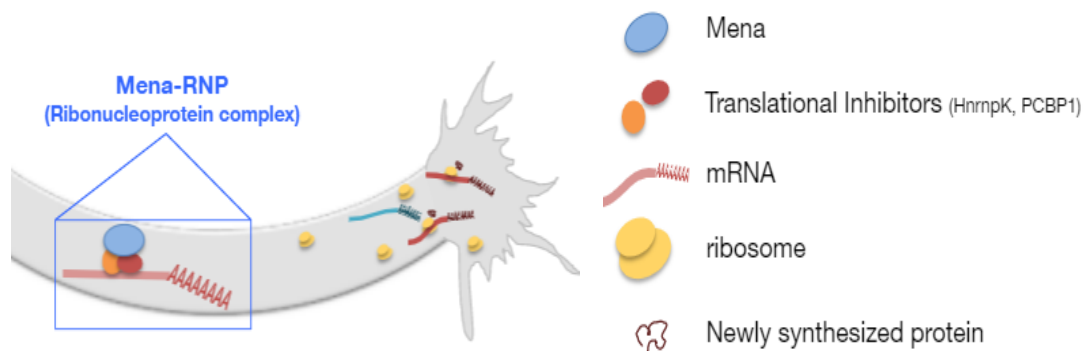


Image 5: The Mena-ribonucleoprotein complex, as suggested by Vidaki et.al., 2017.

Specifically, Mena was shown to regulate the translation of dyrk1a mRNA in growth cones. It is proposed that, possibly by interacting with the two RBPs it was found to be in complex with (HnRNPk and PCBP1), it can control the translation both in

steady-state conditions and upon BDNF stimulation. Dyrk1a is a factor associated with both ASDs and intellectual disabilities such as Down syndrome (Krumm et.al., 2014, O’Roak et.al. 2012). The Mena complex and particularly RBPs HnRNPK and PCBP1 possibly act as translational inhibitors, binding to the 3’-UTR of dyrk1a’s mRNA, and maintaining its translationally inhibited state while in complex with it. Once Mena’s association with HnRNPK and PCBP1 has been disrupted, for example via BDNF stimulation, the mRNA of Dyrk1a is released from its inhibited state.

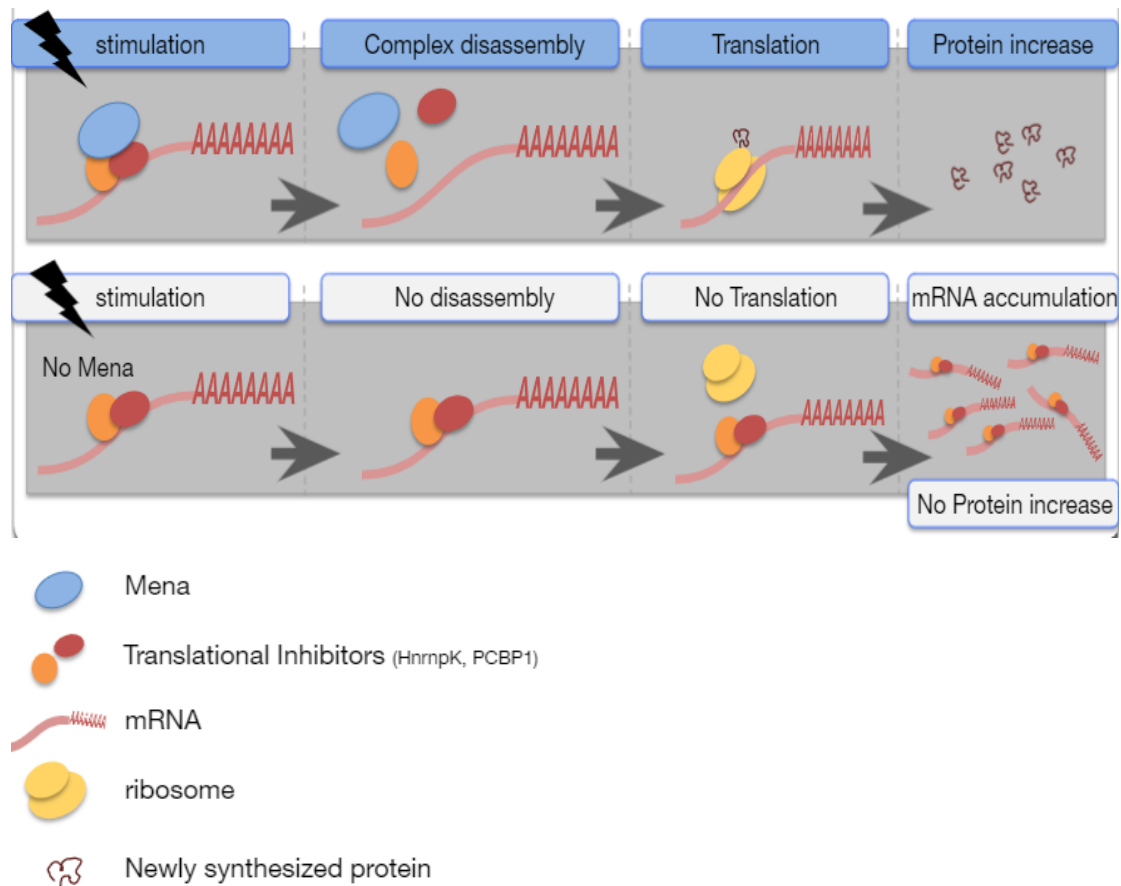


Image 6: Mena’s role in local translation as suggested by Vidaki et.al., 2017.

The Mena-RNP complex has been associated with hundreds of additional mRNAs which show significant differences with locally translated mRNAs that were previously known. One of these mRNAs is the mRNA of Mena itself, which suggests its self-regulation via a feedback loop (Vidaki et.al., 2017). This new evidence suggests a second role for Mena, in localized mRNA translation, via Mena-containing RNP complexes. This role is exclusive to Mena out of all members of its family (Vidaki et.al., 2017).

A.3 Project Outline

For this project, we focused on the distribution of Mena in brain synapses, as few studies have attempted to investigate its potential role there. For this reason, our lab member Manolis Agrymakis Ph.D. initiated a project with the goal of studying the spatio-temporal expression pattern of Mena, particularly in the synaptic compartments of the post-natal mouse CNS. In continuation of this project, this thesis will cover two new timepoints. Previous timepoints that have been studied are the P22 timepoint and the 2mo timepoint. The current thesis focuses on the P15 and P8-10 timepoint.

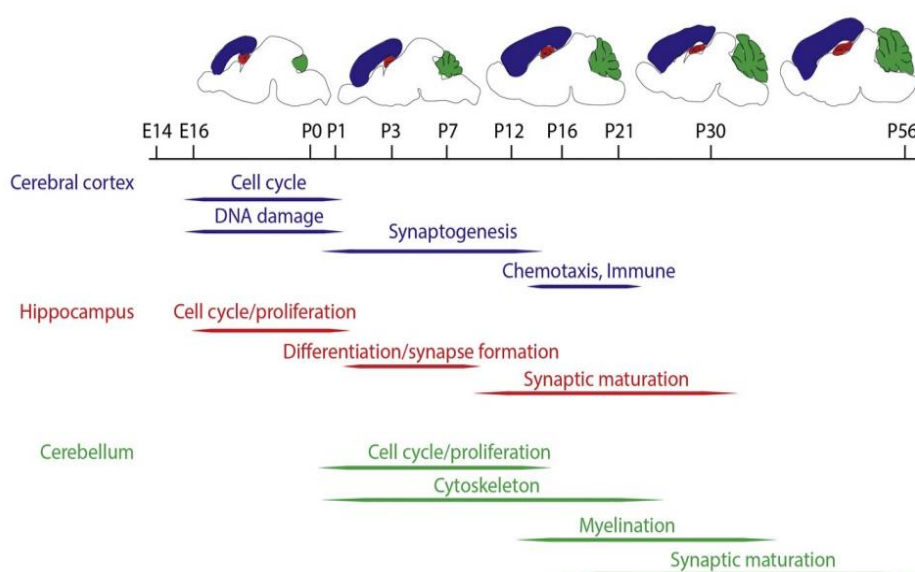


Image 7: Neurodevelopmental processes during early development in the mouse brain, Dillman et.al. 2004.

The reason these timepoints were chosen is that most of the major developmental processes of the central nervous system including synapses are highly active during that period; synaptogenesis, synapse formation and differentiation, synaptic maturation, as well as procedures involving cell proliferation and the cytoskeleton are some of these processes (Dillman et.al., 2004). For that reason, it was decided that the optimal way to continue trying to elucidate the expression pattern of Mena in synapses, and therefore its role, was to study the P8-10 and P15 timepoints.

The areas of the CNS that were studied are the forebrain, the cerebellum, and the spinal cord. The forebrain and the cerebellum were cut sagittally, in slices of 15 μ m and 18 μ m respectively. The spinal cord was cut coronally, in slices of 20 μ m. The areas of interest, as indicated by previous experiments, were: the pyramidal layers from the caudal cortex, the cerebellum, the HF, areas in the ventral and dorsal pons, and the dorsal medulla. The antibodies used for the histochemistry protocols were specifically chosen

and combined in order to specifically mark all major parts of a neuron, allowing us to examine the spatio-temporal distribution of Mena in detail.

For the second part of this project, we focused more specifically on the synapses of the brain themselves, by isolating and studying synaptoneurosomes. Synaptoneurosomes consist of spherical or elongated structures coated by a membrane, sealed off when the axonal termini are fractured during homogenization. For the purposes of this project, synaptoneurosomes were isolated from mice cortices, from P21 mice.

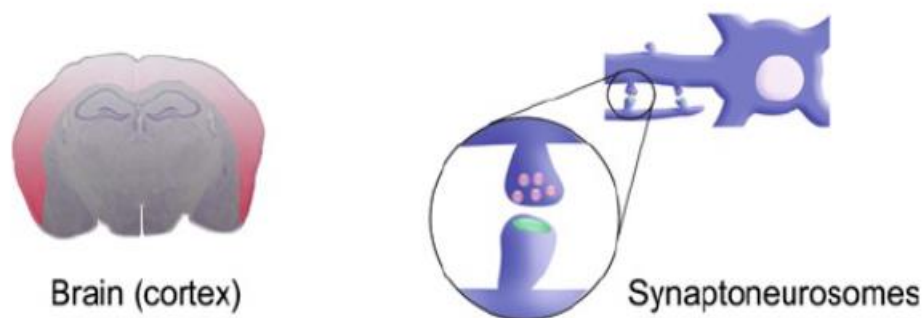


Image 8: De Rubeis, Bagni et.al., 2011

The isolated synaptoneurosomes, consisting of both pre- and post-synaptic terminals, were used for further co-immunoprecipitation and subsequent western-blot experiments. This way, we attempted to study the interaction of synaptic Mena with several different factors, namely: Paralog proteins EVL and VASP, RNP-associated factors such as HnRNPk, PCBP1, and SAFb2, and Mena-associated protein Eef2, a major regulator of translation in mammalian cells (according to the mass spectrometry experiments of Vidaki et.al., 2017).

The main area of interest for this project is Mena's specific synaptic function. We seek to answer questions such as: does Mena's general role in axonal local translation extend to other sub-cellular compartments, namely in synapses? Does it still interact with the same regulators, and if not, what other proteins does it interact with? We hope that, based on these findings, further research can be undertaken to further elucidate Mena's role and provide much-needed answers over its exact molecular function.

B – METHODS

B.1 Immunofluorescence

The mice used are WT C57/BL6. For every timepoint, two different animals were used (preferably male, for consistency with the previous data) to achieve biological replication.

The primary antibodies that were used for these experiments are as follows:

Antibody	Company (Code)	Dilution	Host	Marker type
Mena	Homemade	1/500	mouse	
Mena	Homemade	1/500	rabbit	
MAP2	Millipore/Sigma (AB5622)	1/500	rabbit	dendritic
Synapsin1	Millipore/Sigma (AB1543)	1/500	rabbit	pre-synaptic
2H3 (NF-M)	DSHB (AB_2314897)	1/1000	mouse	axonal
PSD95	ThermoFisher (MA1-046)	1/500	mouse	synaptic
Syngap1	ThermoFisher (PAI-046)	1/500	rabbit	synaptic
Vasp	Homemade	1/500	rabbit	interactor
β 3Tubulin	Cell Signaling (mAB#5568)	1/400	rabbit	neuro/axon.

For the most part, antibodies were used in the following four combinations, for the following purposes:

1. Mena-MAP2: localization of Mena in dendrites.
2. Mena-Synapsin1: localization of Mena in presynaptic compartments.
3. Mena-2H3: localization of Mena in axons.
4. Mena-PSD95 or Mena-Syngap1: localization of Mena in postsynaptic compartments.

The secondary antibodies that were used are as follows:

Antibody	Company (Code)	Dilution	Host
Alexa-Fluor 488	Jackson Laboratories	1/800	mouse
Alexa Fluor 594	Jackson Laboratories	1/800	mouse
Alexa-Fluor 488	Jackson Laboratories	1/800	rabbit
Alexa Fluor 594	Jackson Laboratories	1/800	rabbit

B.1.1 – Cryosections

B.1.1.1 – Perfusion

This entire process takes place in sterilized conditions, under the lab hood. The perfusion mixture used consists of 4% PFA (8% PFA diluted in 2X PBS in a 1:1 ratio). The anesthetic used is a mixture of Ketamine and Xylazine, in a 35:25 ratio, diluted in dH₂O in a 1:1 ratio, for a mouse of roughly 30 grams of weight, the actual amount calculated for each mouse.

- 1) Each mouse is injected endoperitonically with the anesthetic and mounted on the anatomy board.
- 2) The heart is exposed, and a puncture is made on the right atrium. A needle connected to a pump is inserted into the left ventricle of the heart.
- 3) PBS is initially administered to remove excess blood before the introduction of PFA. Afterwards, an equal amount of PFA is administered into the bloodstream of the mouse.
- 4) The brain is carefully removed, dissected, and placed into a container containing ice-cold PFA 4% for 20-30 mins. The spine is removed in a similar fashion, and placed in ice-cold PFA 4% for 20-30 mins.
- 5) After the designated time has passed, the samples are washed with cold PBS and replaced with 10% sucrose, and placed at 4°C overnight (or until samples sink to the bottom).
- 6) The mixture is replaced with a 20% sucrose mixture, and the samples are placed at 4°C overnight.
- 7) The mixture is replaced with a 30% sucrose mixture, and the samples are placed at 4°C overnight.

B.1.1.2 Encasement

The sample encasement mix used consists of 7.5% sucrose, and 15% gelatin.

- 1) The mix is heated at 37 °C, and a petri dish is filled to about 1/3 of its volume.
- 2) The samples are placed on top of the gelatin, after the mixture has cooled down. If there are necessary modifications (such as separating different parts of the brain, or the thoracic/lumbar parts of the SC) they are performed at this point in time.
- 3) The petri dish is filled slowly with the rest of the warm mixture, until the samples are sufficiently covered, and let to solidify.

4) The petri dish is then placed at 4°C for a minimum of one day.

B.1.1.3 Freezing

1) The tissues are removed from the petri dish, enclosed in the solidified mixture, using a blade to cut around the sample, leaving a significant amount of encasing material.

2) The samples are mounted on an aluminium base using OCT.

3) The aluminium base has to be instantly frozen, by submerging it in methylbutane. The methylbutane is carefully temperature-regulated, and the temperature is controlled using dry ice. After each sample, the temperature is once more dropped to the correct range (-40 to -45 °C).

4) The sample is allowed to freeze in methylbutane. Afterwards, it is stored at -80 °C until Cryosectioning is performed.

B.1.1.4 Cryosectioning

For this process, the cryotome has to maintain a temperature of -25°C.

1) The sample is mounted on top of the metallic base of the cryotome, and the position is secured. The metallic base is adjusted for the correct alignment of the sample.

2) The cryosectioning begins, and slices of encasement material are sectioned off until the actual sample has been reached.

3) After reaching the sample, there needs to be a lot of caution as to the alignment of the sample, which will affect the slides. If necessary, a digital or other type of anatomy atlas of the area can be consulted to make sure that the slides created are the desired type.

4) The slides can then be placed on subbed slides.

5) The slides can be stored at -20°C.

The cryotome model used is the Leica CM1860UV.

B.1.2 Immunohistochemistry

1) The slides that will be used are removed from storage and left for 10-15 minutes to acclimate to the temperature of the room, inside their case. The slides are then removed and let to dry.

- 2) The borders of the slides are covered in dackopen. If a slide needs to be sectioned, dackopen can be used.
- 3) Post-fixation: 10 min in 100% cold Acetone at -20 °C.
- 4) 3x5min rinses are performed with PBS at RT.
- 5) Permeabilization: incubation for 15 min in PBS containing 0.3% TritonX.
- 6) Blocking: The blocking solution used consists of 10% NGS and 3% BSA in PBS containing 0.3% TritonX. Blocking lasts 2 hrs at RT (about 300µl used per slide).
- 7) Incubation with primary antibodies: The solution used to dilute the antibodies consists of 5%NGS, and 1%BSA in PBS containing 0.1% TritonX. The antibodies are left ON, at 4 °C (about 200 µl used per slide).
- 8) 3x10min rinses with TBS containing 0.01% Tween at RT.
- 9) Incubation with the secondary antibodies: duration of 2 hrs, at RT, and in the dark. The antibody solution used consists of 5% NGS, and 1% BSA in PBS containing 0.1% TritonX.
- 10) 3x10min rinses with TBS containing 0.01% Tween at RT. These rinses are performed in the dark.
- 11) 1x5 minute rinse with PBS.
- 12) DAPI staining: In a concentration of 1:1500, left for 5 minutes in the dark.
- 13) 3x5min rinses, in the dark, with TBS containing 0.01% Tween at RT.
- 14) Mounting is performed using Mowiol as a medium. For each slide, approximately 65µl of Mowiol were used.
- 15) The slides are stored at 4 °C, and sealed the next day, after Mowiol has solidified. If they are not meant for immediate use, the slides can be stored at -20 °C.

B.1.3 Imaging and Data Analysis

The imaging was performed using a DMI8 Leica TCS-SP8 confocal microscope. The editing of the pictures retrieved was accomplished utilizing the image software LAS-X, as well as the software ImageJ Fiji.

B.2 – Synaptoneurosomes

B.2.1 – Synaptoneurosome Isolation

Protocol used: “Identification and Characterization of Protein Complexes from Brain and Synaptoneurosomes: Heterogeneity of Molecular Complexes in Distinct Subcellular Domains”, by De Rubeis, Bagni et.al. The procedure can be summarized in the following picture:

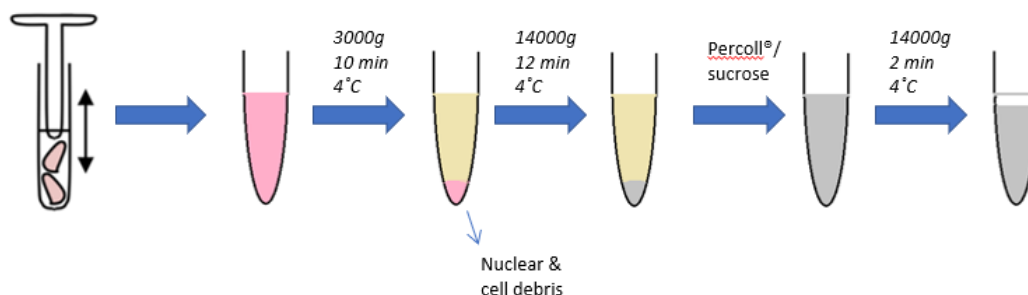


Image 9: The SN isolation protocol (De Rubeis, Bagni et.al., 2011).

The protocol, in some greater detail, is as follows:

1. Euthanization: The mice needed are euthanized by cervical dislocation. (For the most part, mice were used in sets of 4, to reach the quantity needed for a co-IP experiment.)
2. Homogenization: The cortices were dissected and then homogenized. Homogenizing buffer: 0.3M Sucrose, 100mM NaCl, 1mM EDTA, 1mg/ml BSA, 5mM HEPES, with a PH of 7.4. For every 4 mice, 6.6 mL of Homogenizing buffer were used. The pestle used was a Whitton glass pestle type B, and 10 up-and-down strokes were performed with a twisting motion.

3. First High-Speed Centrifugation: The samples were centrifuged at 3.000g(7.600rpm) for 10min at 4 °C, using a 70.1Ti Rotor, that is being stored at 4 °C for better cooling of the samples during the high-speed centrifugation. The supernatant was then centrifuged anew.

A small amount of the supernatant was stored, as brain input control for the co-immunoprecipitation experiments.

4. Second High-Speed Centrifugation: The samples were centrifuged at 14.000g (14.300rpm) for 12min at 4 °C, using the 70.1Ti Rotor again. The supernatant was discarded, and the pellet containing the synaptoneurosomes was further processed.

5. The pellet was gently resuspended in Krebs Ringer Buffer (370µl for every 4 cortices) containing protease inhibitors (PIs). KRB: 140mM NaCl, 5mM KCl, 5mM glucose, 1mM EDTA, 10mM HEPES, with a PH of 7.4. (PIs used: Roche, Protease inhibitor cocktail tablets, 11697498001, 1 tablet per 50ml of KRB).

300µl of percol were used for each sample

6. First Low-Speed Centrifugation: after gently flicking the mix, the tube was centrifuged at 14.000 for 2 min at 4 °C.
7. The synaptoneurosomes are found on the top surface of the gradient. The underlying solution was removed, and the remaining synaptoneurosomes were gently resuspended in 670µl of KRB.
8. Second Low-Speed Centrifugation: The samples were centrifuged at 14.000rpm for 30sec at 4 °C. The supernatant was discarded, and the pellet containing the synaptoneurosomes gently resuspended in 400µl of KRB with PIs. If the samples are meant to be used immediately for co-immunoprecipitation, the pellets were resuspended in an equal amount of mild RIPA buffer containing PIs.
9. Calculation of protein concentration: The samples' protein concentration was calculated using the Bradford assay. (For each 1ml cuvette: 800µl dH2O, 200µl Bradford buffer, 5µl sample). The optical density was calculated at 595nm, and properly calibrated for each sample using a negative control. The equation used to calculate the protein concentration is: $y=0.2501x+0.0632$, where y are the OD values and x the protein concentration in µg/µl.
10. The samples can then be used immediately or stored long-term at -80 °C.

Note: Although there were significant efforts for the mice's age to be kept consistent, it is impossible to verify the exact birth date of the mice, as they were provided to us by a third-party service. We calculate that there could be a 1-2 day upwards margin of fault (mice used in these experiments could be up to 23 days of age).

B.2.2 Co-Immunoprecipitation

Co-immunoprecipitation was performed using the isolated synaptoneurosomes. For each tube, a total of 500µg of protein were used, and the protein concentration calculated using the Bradford array. Two different protocols were tested, a 1-day protocol, and a 2-day protocol. After careful deliberation, the 1-day protocol was selected, as it showed greater co-precipitation, on top of requiring less time. Both protocols are described below.

1. Magnetic Bead preparation: 40µl of Ab-crosslinking protein-G magnetic beads (Biorad #161-4023) are used per 1.5 mL tube (low adhesion). The beads are washed with 1mL PBS.
2. Primary antibodies: For Mena IP, 5µl of Mena antibody were used (homemade, Frank Gertler) per tube. For the technical negative control, 13,5µl of IgG2a antibody were used (Abcam, ab18413) per tube. The quantities were optimized for 500µg of protein for each tube, and the antibodies diluted in 1ml of PBS.

For the 2-day protocol: The beads are incubated with the antibodies for 2-4 hrs, at 4 °C, on a rocker. For optimal results, the beads were allowed to incubate for the entire 4-hour span.

For the 1-day protocol: The beads are incubated with the antibodies for 1 hr at RT, on a rocker.

The beads were then washed 3x with PBS, and 1x with mild RIPA buffer.

3. Introducing the lysate: 500 μ g of protein are loaded on each tube. Then mild RIPA buffer containing PIs is added until a quantity of 500 μ l has been reached. Mild RIPA buffer: 150mM NaCl, 1% TritonX-100, 0.5% DOC, 50mM Tris-HCl with a PH of 8. (PIs used: Roche, Protease inhibitor cocktail tablets, 11697498001, 1 tablet per 50ml of KRB)

For the 2-day protocol: The beads are incubated with the lysate ON, at 4 °C, on a rocker.

For the 1-day protocol: The beads are incubated with the lysate for 2 hrs, at RT, on a rocker.

A calculated quantity of lysate containing 5% of the loaded protein was kept for input control.

Where standard lysis was needed (for example, in using whole brain to compare the two protocols) the technique that was used is as follows: Half a brain of an adult mouse is homogenized in 1.5 ml of mild RIPA buffer, containing PIs (Whitton B glass pestle, 14 ounces, 4x up and down using a syringe with a 27G needle, 4x up and down using a syringe with a 23G needle). The lysate was let to rest for 15 min, and then centrifuged at 15.000rpm for 15min at 4 °C. The supernatant is then used in the same way as the SNs lysate after the final pellet is resuspended in mild RIPA buffer.

4. A small quantity of the supernatant was kept to be used in the subsequent western blot experiment.

5. 3x washes with mild RIPA buffer were performed, and then the beads, SPN and input samples were prepared for Western blot electrophoresis.

B.2.3 Western Blot Electrophoresis

1. Preparation of the samples:

The elution buffer is as follows: 2x or 4x laemmli, 10x DDT, optional: mild RIPA buffer with PIs as needed for the correct volume). More specifically, the amounts used were:

For elution of the beads: 15 μ l 2x laemmli, 3 μ l 10x DDT, 12 μ l of mild RIPA buffer for a final volume of 30 μ l.

For the supernatant: 20 μ l of supernatant kept, 8 μ l 4x laemmli, 3 μ l 10x DDT.

For the IP input and the brain input: the volume of the lysate used depends on the concentration, the input must contain 25 γ of total protein. 2x or 4x laemmli, 10x DDT and mild RIPA buffer are added as needed to reach a total volume of 30 μ l.

The tubes were heated at 95 °C (10 min for the beads, 5 min for the rest of the samples). After this, the tubes can be safely stored at -20 °C or used for immediate Western blot electrophoresis.

2. Preparation of the gel:

The samples are run on an acrylamide 10% stacking and running gel. The ingredients for a single gel are:

Ingredients	Running Gel	Stacking Gel
H2O	2,25ml	2,2ml
6,8Tris/8,8Tris respectively	3,75ml	0,5ml
SDS	100 μ l	80 μ l
Acrylamide	3,3ml	0,67ml
TEMED	8 μ l	6 μ l
APS	110 μ l	50 μ l

The running buffer is prepared first, poured into the glass plates, and let to solidify. 2-propanol can be used to avoid bubbles forming on top of the gel, and then removed before the introduction of the stacking buffer. Once the running gel has solidified, the stacking buffer is introduced, and a comb with the desired number of wells added. Once the gel is solid, electrophoresis can begin.

3. Running:

The electrophorator is filled with running buffer, and the samples as well as an appropriate protein ladder are loaded into the wells. The voltage is set at 90V until the samples reach the end of the stacking gel, and then set anywhere between 120-140V. For the majority of the experiments run, the voltage was set between 130-135V.

4. Transfer:

After running was completed, the gels were removed from the electrophorator, and then separated from the glass plates. The gels were placed inside the cassette along with a piece of nitrocellulose membrane (GVS Life Sciences, 1215458), and carefully stacked together using Wattman paper and sponges. The bucket was filled with cold transfer buffer and the electrophorator set at 0.35A for 2 hrs.

5. Blocking: After the transfer is finished, the gels are discarded and the membranes incubated with 5% nonfat dried milk diluted in TBS-Tween 0.1% for an hour, on a rocker.

6. Primary antibodies: The membranes are incubated with the respective antibody per membrane piece, ON, at 4 °C.

Primary antibodies used:

Antibody	Company (Code)	Dilution	Host
Mena	Homemade (Frank Gentler)	1/500	mouse
Mena	Homemade (Frank Gentler)	1/500	rabbit
Vasp	Homemade (Frank Gentler)	1/2.000	rabbit
Safb	AbCam (ab8060)	1/1.000	mouse
eEF2	Cell Signaling (2332)	1/1.000	rabbit
HnrnpK	Cell Signaling (4675)	1/1.000	rabbit
PCBP1	MBL (RN024P)	1/1.000	rabbit
EVL	Homemade (Frank Gentler)	1/1.000	mouse
b-actin	Cell Signaling (4870)	1/1.000	rabbit

7. Secondary antibodies: After 3x10min washes are performed with TBS-Tween 0.1%, the membranes are incubated with the secondary antibodies for 1hr at RT on a rocker.

Secondary antibodies used:

Antibody	Company (Code)	Dilution	Host
Goat Anti-mouse HRP	Homemade	1/5.000	mouse
Goat Anti-rabbit HRP	Homemade	1/5.000	rabbit

8. Visualization of the results:

After 3x10min washes are performed with TBS-Tween 0.1%, the membranes are treated with ECL (about 500µl per membrane) and the results analyzed by enhanced chemiluminescence. The software used to analyze these results is ImageLab.

C – RESULTS AND DISCUSSION

C.1 Immunofluorescence

For this part of the project, confocal pictures from the immunohistochemistry experiments will be listed from both timepoints (P8-10 and P15). For each timepoint, two duplicate sets of experiments were performed for each area of interest (forebrain areas, cerebellum, spinal cord) using different mice, to achieve biological and technical duplicity. All the mice and antibodies used are listed in the respective table in the supplementary material section. Negative control experiments were performed for each set with only secondary antibodies, and results were carefully compared during picture acquirement and compilation, to ensure that the data shown is significant. Immunostaining was also performed on a set of Mena KO cryosections, as a second level of negative control.

C.1.1 Expression pattern of Mena in P8-10 mouse NS

Between days 8 and 10 of the CNS development in mice, several important neurodevelopmental processes take place, including synaptogenesis, synapse differentiation and formation, cell cycle and proliferation, and cytoskeleton formation. Due to Mena's dual nature, and possible implication in most of these processes, we theorize that its expression pattern will be highly pronounced in most parts of the CNS.

In order to study the spatiotemporal analysis of Mena in the forebrain, sagittal cryosections were used, in order to expose structures of interest such as the different cortex layers (CrxL5 and CrxL2/3) in the Prefrontal Cortex (PFC) and the caudal Cortex (cdCrx), the hippocampus (Hp), the Corpus Callosum (CC), the olfactory bulbs (OB), the Thalamus (Th) as well as the Hypothalamus (HTh). These areas of interest were determined based on previous work from our lab in coronal sections of P22 and 2m.o. mouse brains; its expression pattern was found to be pronounced in these areas, and further research in diverse timepoints was deemed necessary. The Allen Mouse Brain Atlas was used for the identification of these areas during confocal microscopy, and nissl-stained cryosections are used in each figure as reference.

As shown in Images 10a, 10b, and 10h, the cortex shows strong Mena immunoreactivity, with Mena showing a pronounced expression in the cell bodies of the large neurons in the fifth pyramidal layer (L5). Mena appears to be primarily distributed on the surface of cdCrx (caudal Cortex) L5 cells as well as on their axon initial segments, and in some cases in further lengths of these axons (10c, 10e). Axon initial segments (AISs) generate and shape the action potential before it is propagated along the axon, and are thus characterized by a unique molecular profile (Leterrier et.al., 2018). AISs are areas that have to quickly adapt to developmental and physiological conditions, and would theoretically have a higher need for the adaptability that local translation provides.

P8/10 Forebrain – Cortex

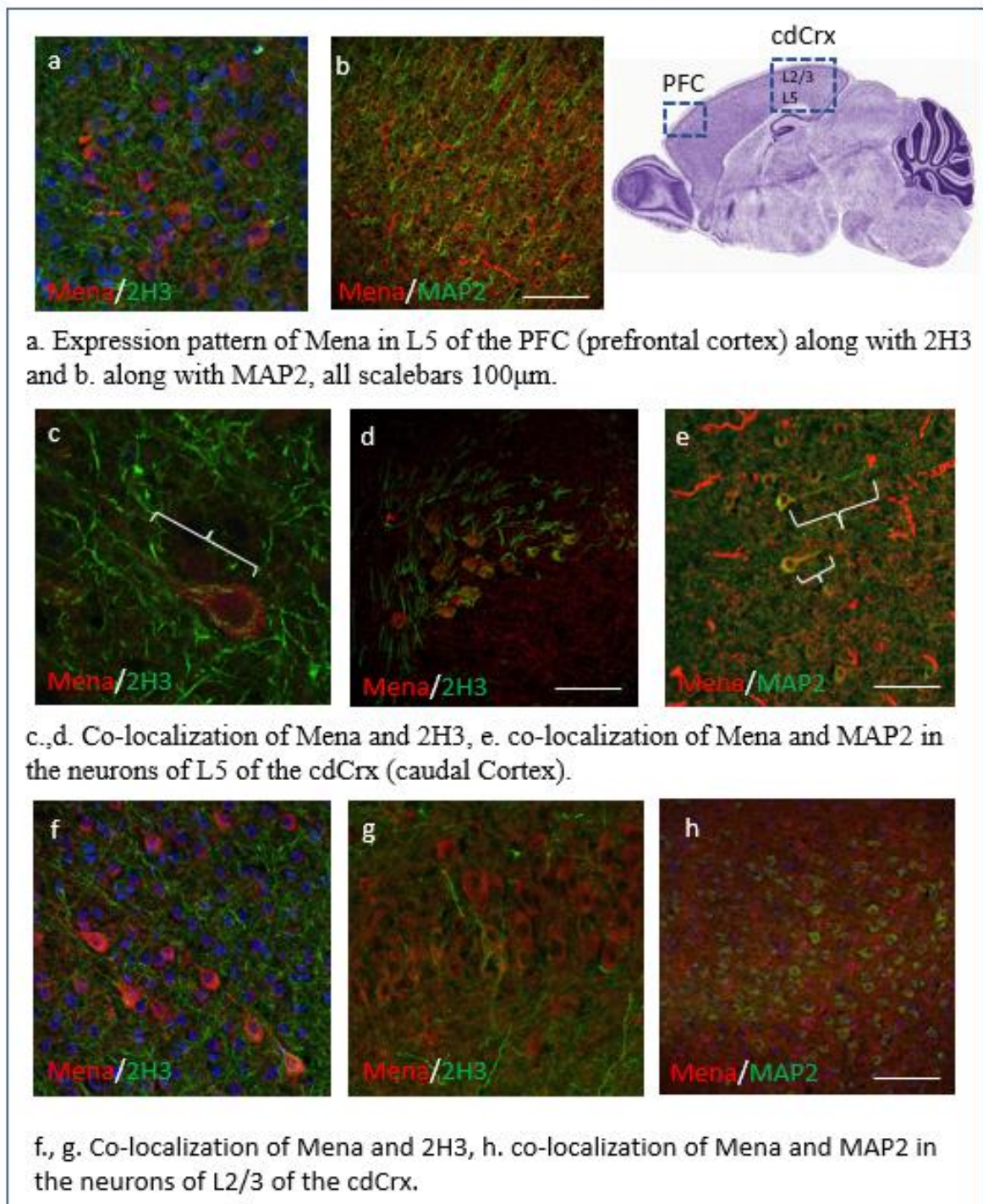


Image 10: Co-localization of Mena and dendritic marker MAP2 as well as axonal marker 2H3 in layers 2/3 and 5 of the prefrontal and caudal cortex of P8-10 mice.

Mena's expression appears to be increased in the cortex in general, both in L2/3 and L5 layers. Co-localization was observed with both dendritic marker MAP2 as well as axonal marker 2H3. The pre-synaptic marker Synapsin1 and post-synaptic marker PSD95 gave no reliable, duplicated results. In other timepoints such as P22, the signal of Mena was observed as reduced in layers 2/3, but no such thing was observed for

the P8-10 timepoint. The different neurodevelopmental processes that were mentioned above may be exceedingly active during this time, and this is what causes this uniform expression pattern of Mena throughout the different cortex layers. The key differences between these timepoints could offer an interesting angle for future investigation.

P8/10 Forebrain – Hippocampal Formation

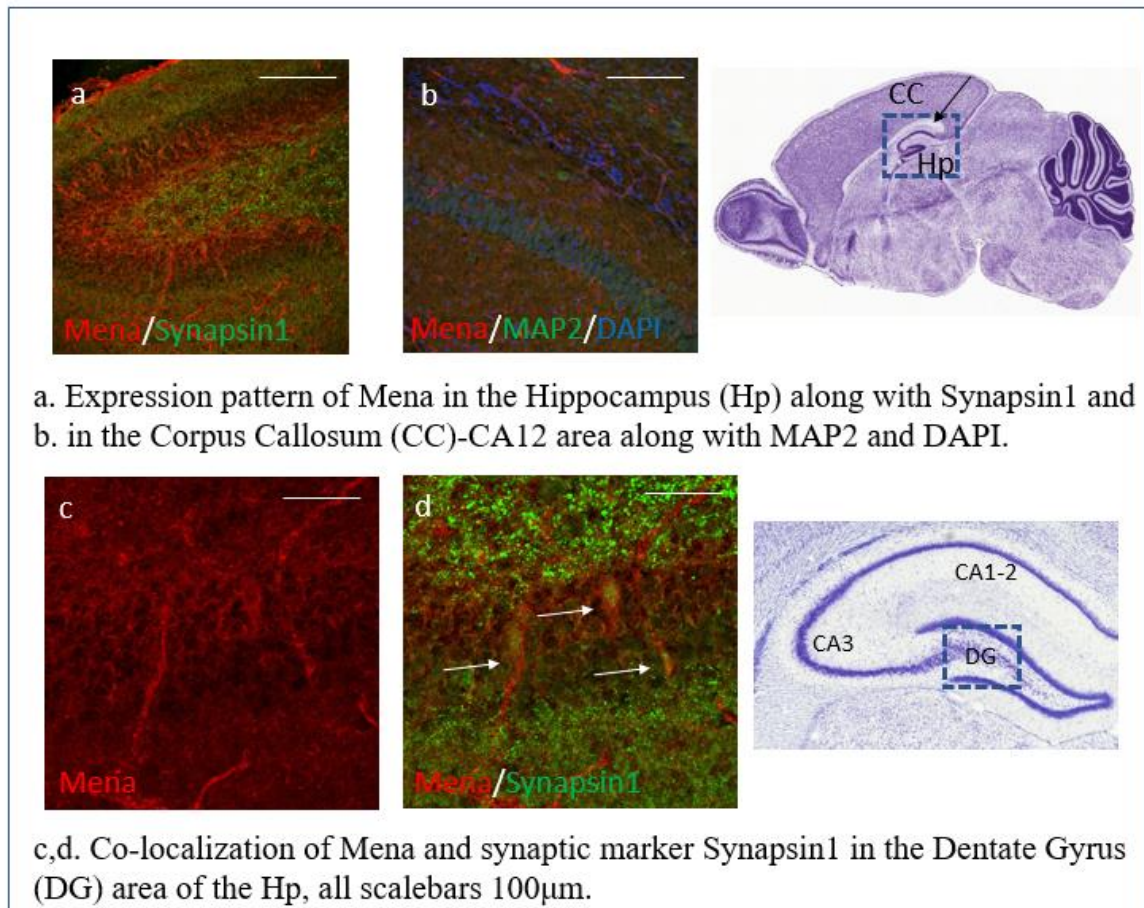


Image 11: Expression pattern and co-localization of Mena with synaptic markers in the areas of the Hippocampal formation and the Corpus Callosum of P8-10 mice.

In the Corpus Callosum (CC), Mena's distribution was not as prominent as in the Cortex, and seemed to not be visible in the CC cell's axons (10b). The Hippocampus (Hp) displayed a stronger Mena immunoreactivity, but not as strong as in the Cortex.

The areas observed were the formations of the Dentate Gyrus (DG) as well as the Cornu Amomum (CA) areas which encompass the trisynaptic circuit: CA1-2, and CA3. Mena's colocalization with pre-synaptic marker Synapsin1 was noticed in a couple of neurons of the DG (11d). Mena was observed in both the main bodies of these neurons

P8/10 Forebrain – Olfactory Bulb

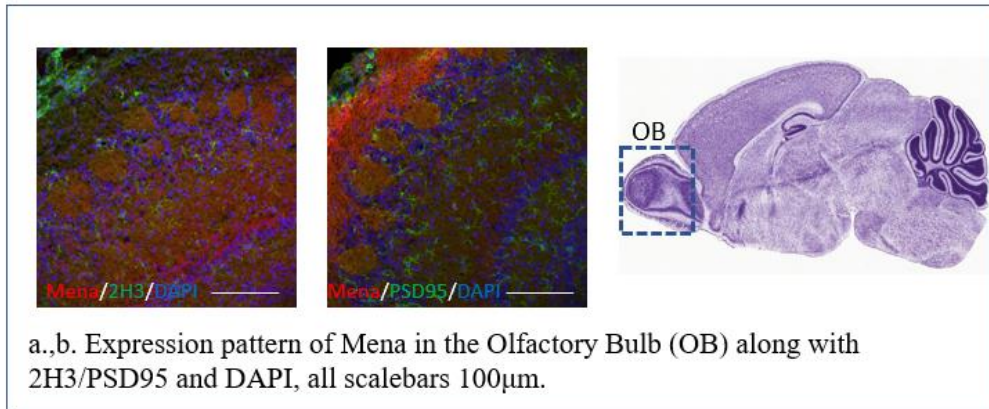


Image 12: Mena's P8-10 Olfactory Bulb (OB) expression pattern.

P8/10 Cerebellum

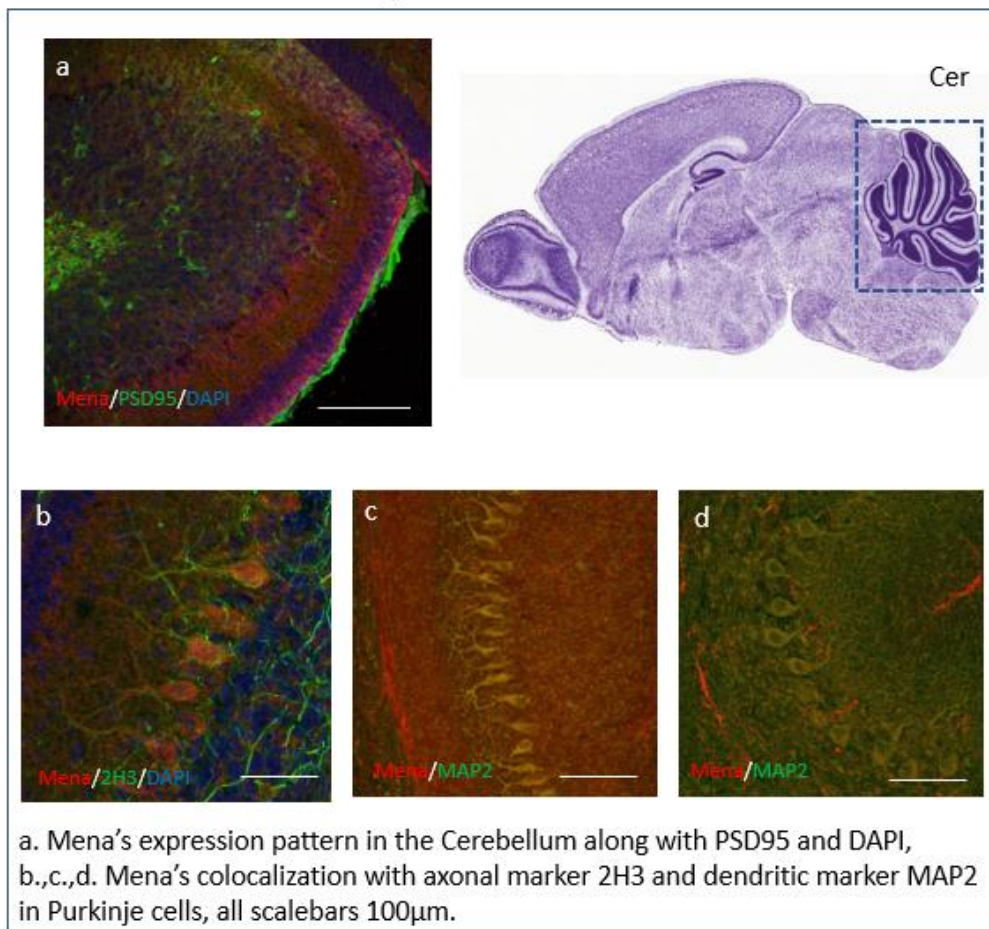


Image 13: Mena's localization in the P8-10 Cerebellum (Cer).

as well as their axons. This data is consistent with the P22 timepoint, in which Mena was also observed to co-localize with Synapsin1 in DG neurons. Mena's co-localization with Synapsin1 was also observed in the interior of the DG. The CA areas presented a similar immunoreactivity signal pattern with the entire Hippocampal formation.

Mena presents a pattern of strong immunoreactivity in the entire Olfactory Bulb (OB). Some partial co-localization is observed, with both axonal and post-synaptic markers, as shown in the figures in Image 12. However, no specific synapse co-localization was observed for Mena and either of the 4 different markers (Synapsin1, MAP2, 2H3, PSD95).

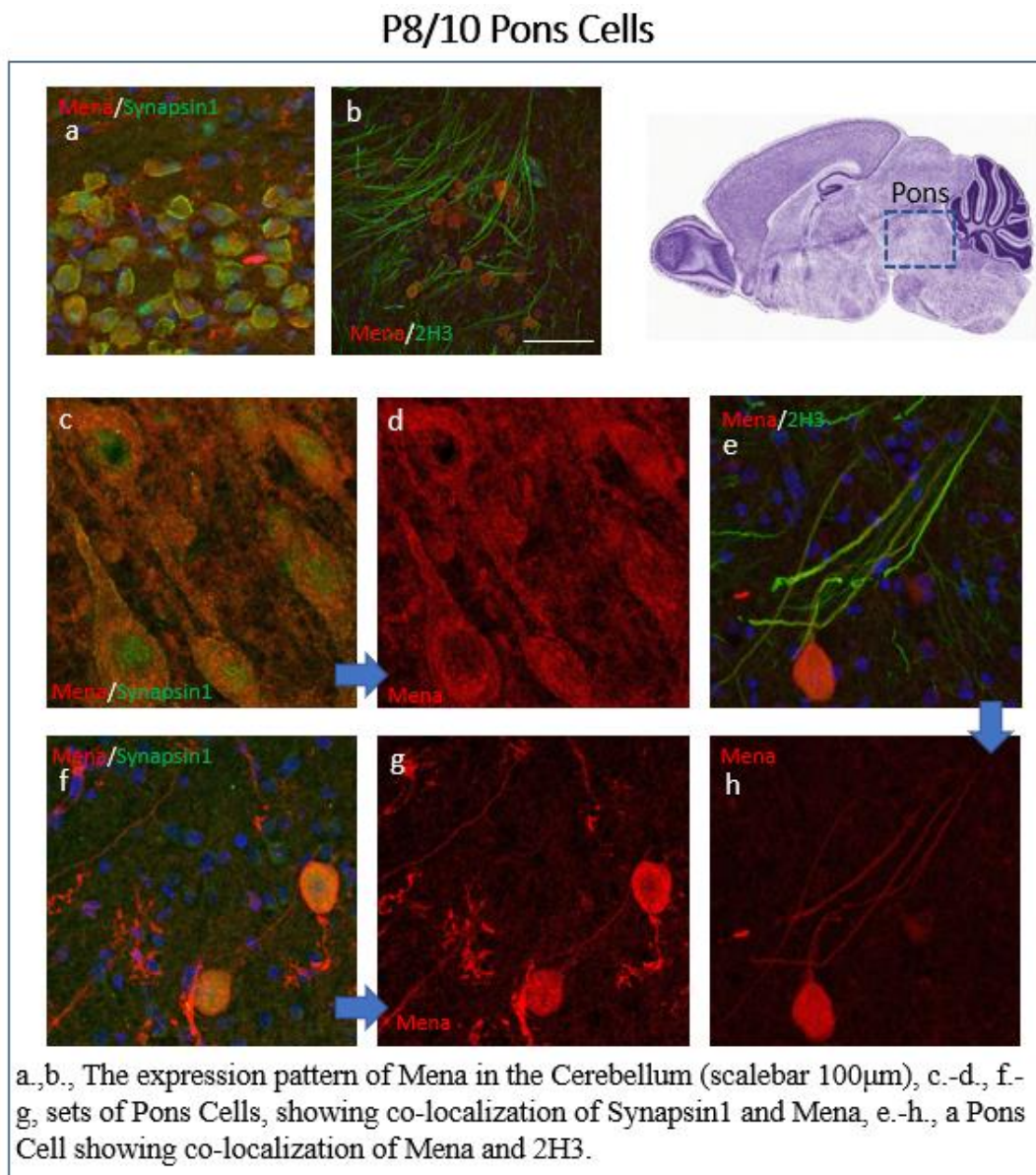


Image 14: Mena's localization in the P8-10 Pons Cells area.

In the Cerebellum, an overall increased signal of Mena was observed, compared to other brain structures (Image 13). This signal was mostly observed in the Purkinje cell layer (PCL). Both the cell body and axons/dendrites were strongly stained with the Mena antibody, and showed distinct co-localization with synaptic markers (13b,c,d). These observations are consistent with the P22 timepoint, while this strong immunostaining pattern ceases at the 2m.o. timepoint. Reduced Purkinje cell neuroplasticity has been found to be connected with autism brain disorders (ASDs) in children (Piochon et.al., 2014). This might be a possible avenue for future research regarding Mena's connection to ASDs.

P8/10 Medulla

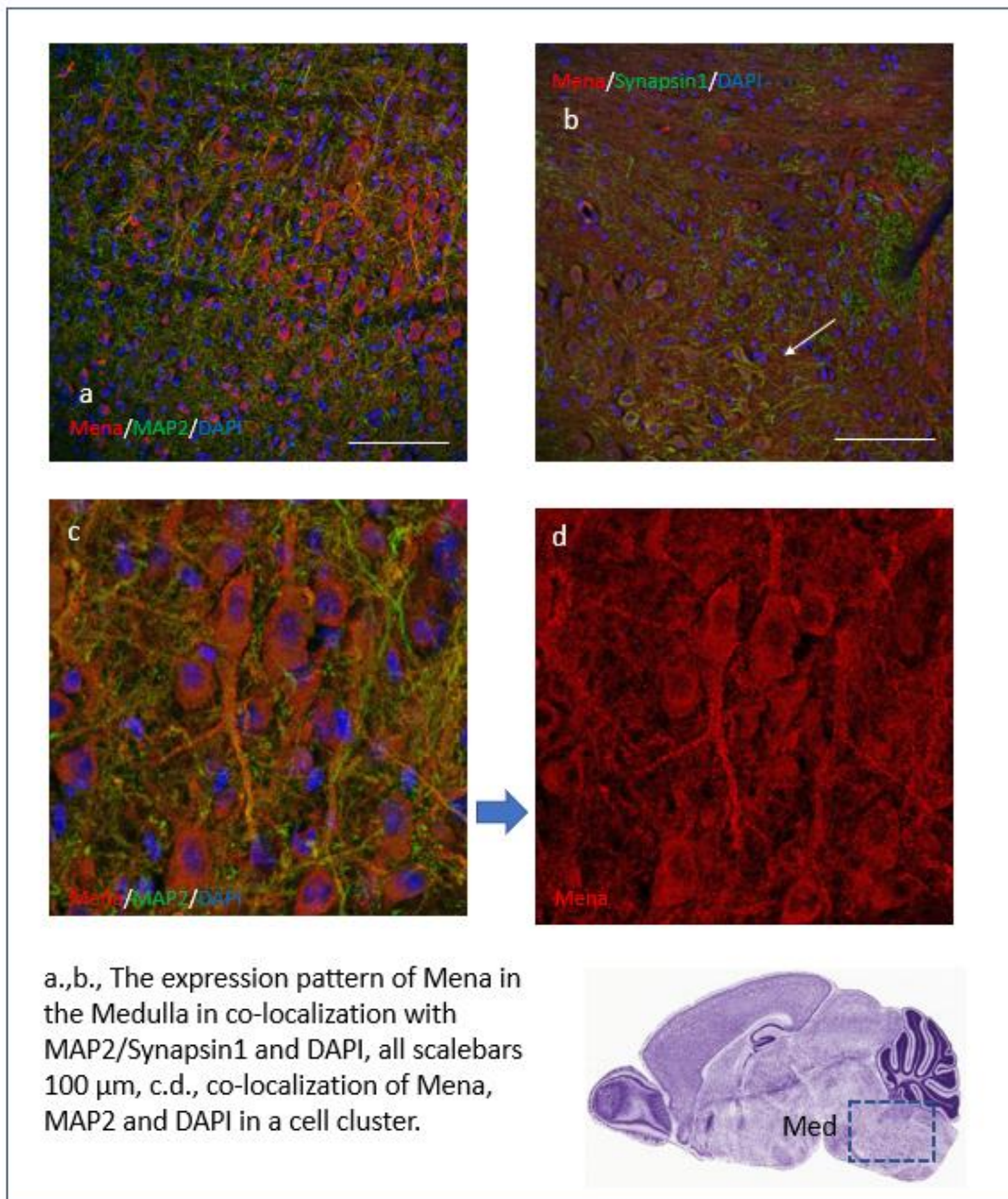


Image 15: Mena's localization in the P8-10 Medulla.

In the Pons area, several cells were consistently observed, in which Mena's immunostaining signal was particularly strong. Mena was observed both in the cell bodies and axons of developing neurons, co-localized with pre-synaptic marker Synapsin1 and axonal marker 2H3.

Similarly to the Pons area, the Medulla shows strong immunoreactivity to Mena, and Mena was observed in neurons, both in the main cell body as well as in axons and dendrites (15c,d). Mena showed co-localization with both presynaptic and dendritic markers (15a,b,c).

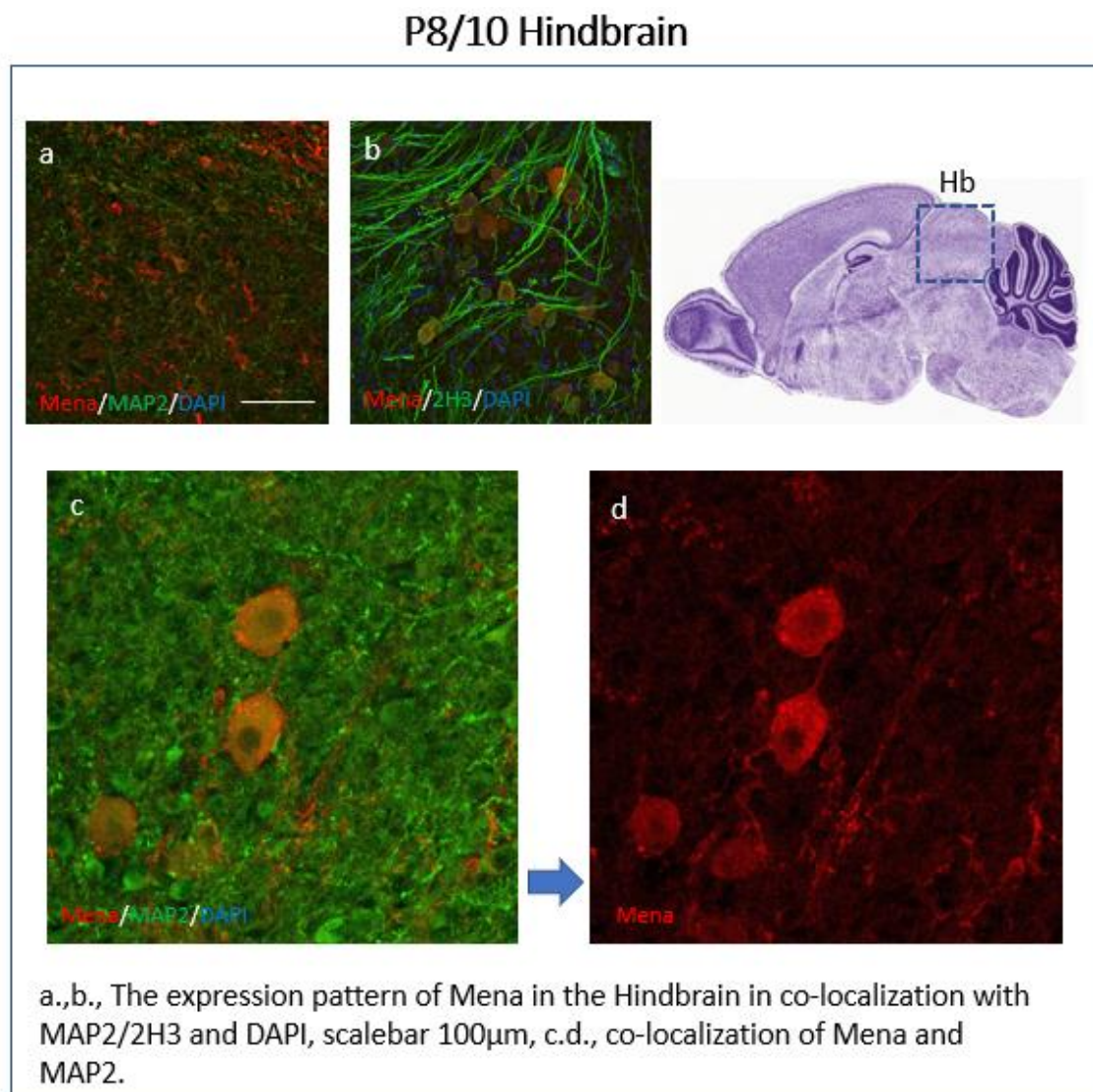


Image 16: Mena's localization in the P8-10 Hindbrain area.

Mena's expression pattern in the hindbrain area was not as strong as in other areas of the caudal brain, there were however multiple cells observed with clear Mena staining. In Images 16a and 16b, Mena's colocalization with markers MAP2 and 2H3

is observed, and in Images 16c and 16d, there is a connection between a neuron and what appears to be a glial cell, with a strong Mena signal between the two.

P8/10 Spinal Cord

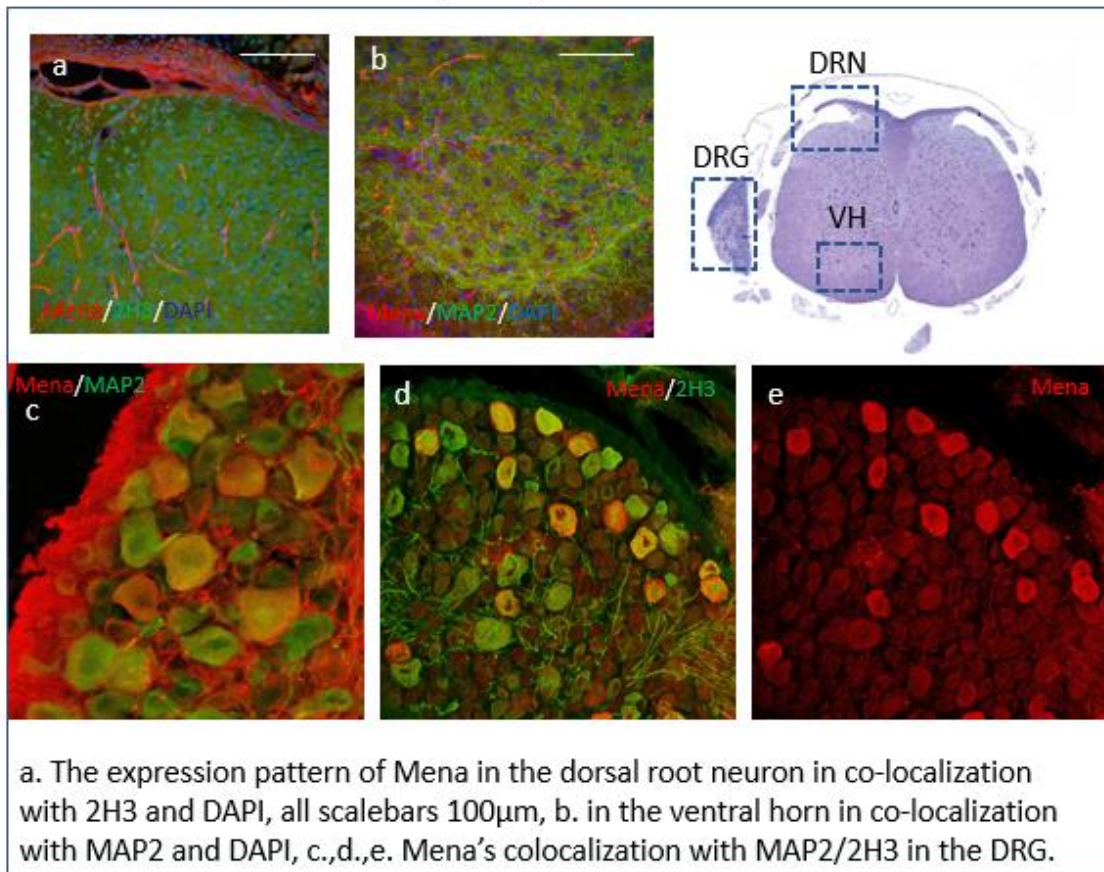


Image 17: Mena's localization in the P8-10 Spinal Cord.

In the Spinal cord, Mena's IF staining was examined in both thoracic and lumbar slices, with no notable differences observed. Mena's signal was most pronounced in the DRGs (dorsal root ganglions), which contain the bodies of the primary sensory neurons in charge of transmitting signals from peripheral sensory receptors to the spinal cord (17c,d,e). The dorsal root nerve (DRN) shows an increased Mena immunoreactivity pattern, with Mena staining axons both in the DRN and its peripheral extension (17a). In comparison, the ventral horn (VH) area shows a lower immunoreactivity, however, cell bodies with co-localization of Mena and MAP2 can still be observed (17b).

C.1.2 Expression pattern of Mena in P15 mouse NS

In concert with the timepoint P8-10, two duplicate sets of experiments were performed for each area of interest (forebrain areas, cerebellum, spinal cord) using different mice, to achieve biological and technical duplicity. Negative control experiments were performed to test the specific staining of secondary antibodies, and the results were only taken into consideration after careful comparison with their corresponding negative controls.

P15 Forebrain – Crx, Hp, OB

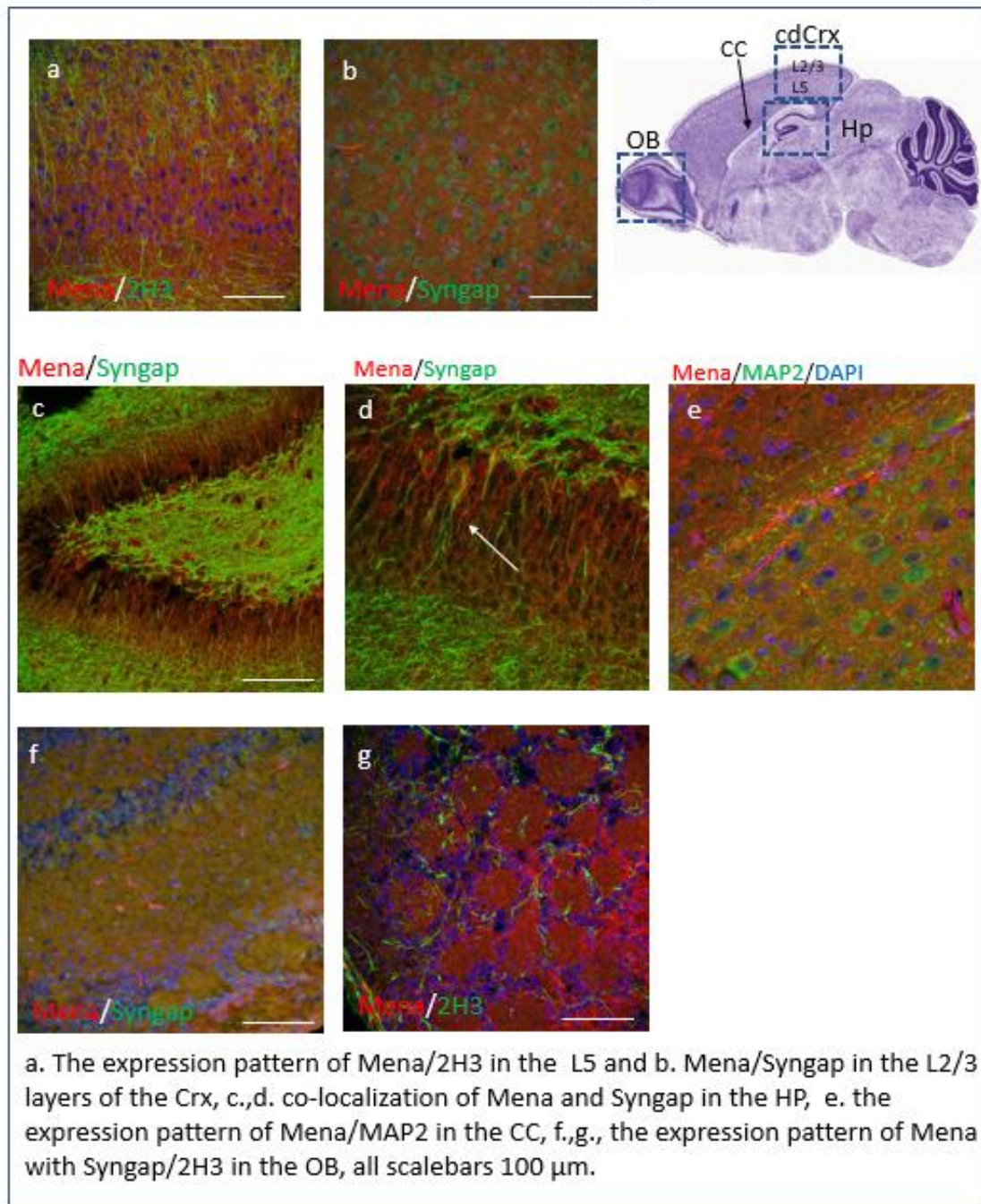


Image 18: Mena's expression pattern in the forebrain areas of P15 mice.

P15 Cerebellum

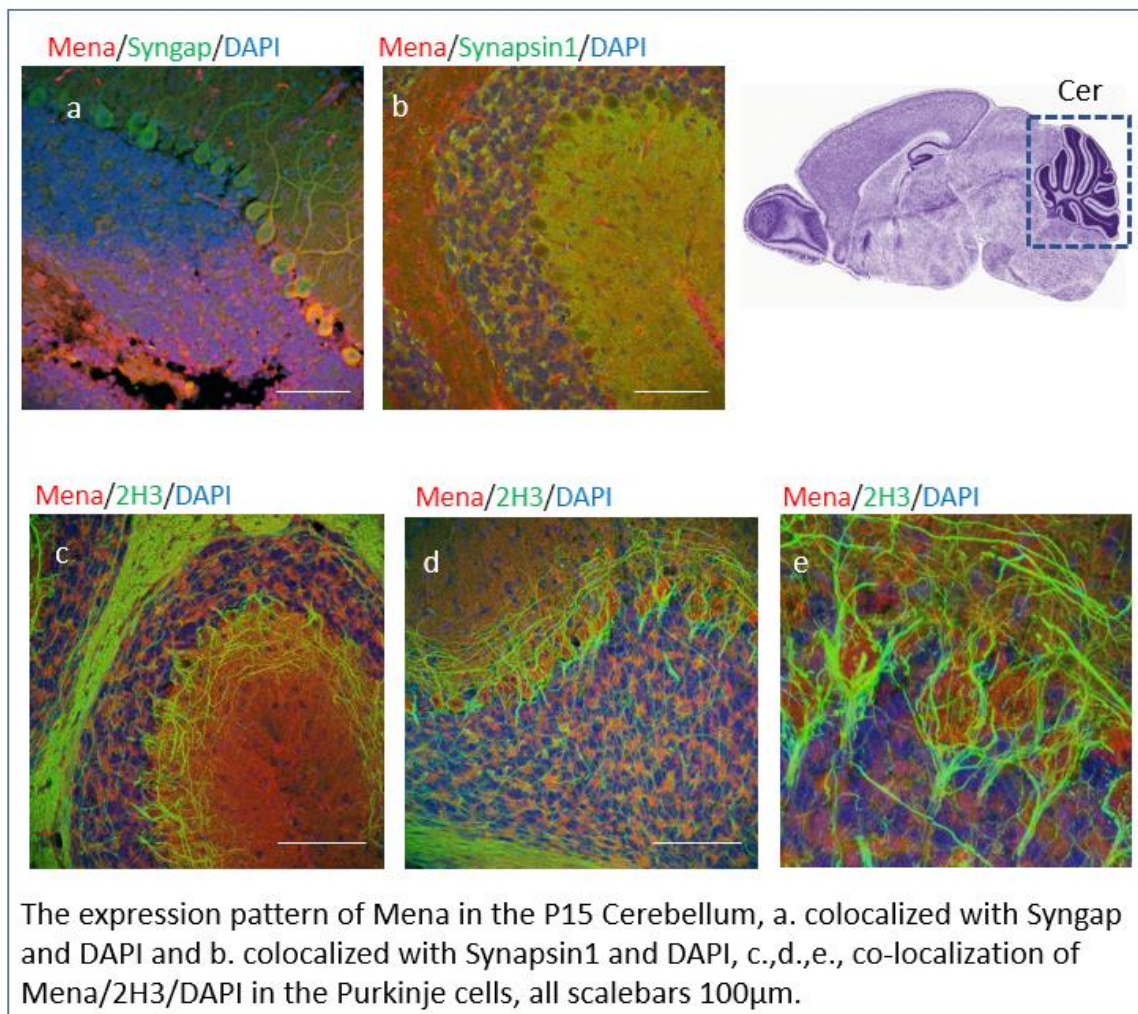


Image 19: Mena's expression pattern in the P15 Cerebellum.

On the 15th day of postnatal development, important neurodevelopmental processes have either ceased completely or are rapidly coming to a close. Such processes are the synaptogenesis in the cerebral cortex, synapse differentiation and formation in the hippocampus, and cell cycle, proliferation, and cytoskeleton processes in the cerebellum. Taking into account Mena's well-known role of actin dynamic regulation as well as the theorized role of local translation regulation, it is believed that Mena's expression profile and co-localization with synaptic markers will be less pronounced in this timepoint compared to the P8-10 timepoint.

This divergence was indeed observed while studying the forebrain areas of P15 mice. Beginning with the forebrain areas, and as shown in Images 18a and 18b, Mena's expression pattern is less pronounced in the L2/3 and L5 layers of the Cortex, with no notable co-localization in synapses. Although two different mice and a number of different slides were tested with a variety of different markers, this observation remained consistent. On the contrary, the hippocampal formation presented a similarly pronounced pattern of Mena immunostaining, with co-localization of Mena and

P15 Pons Cells

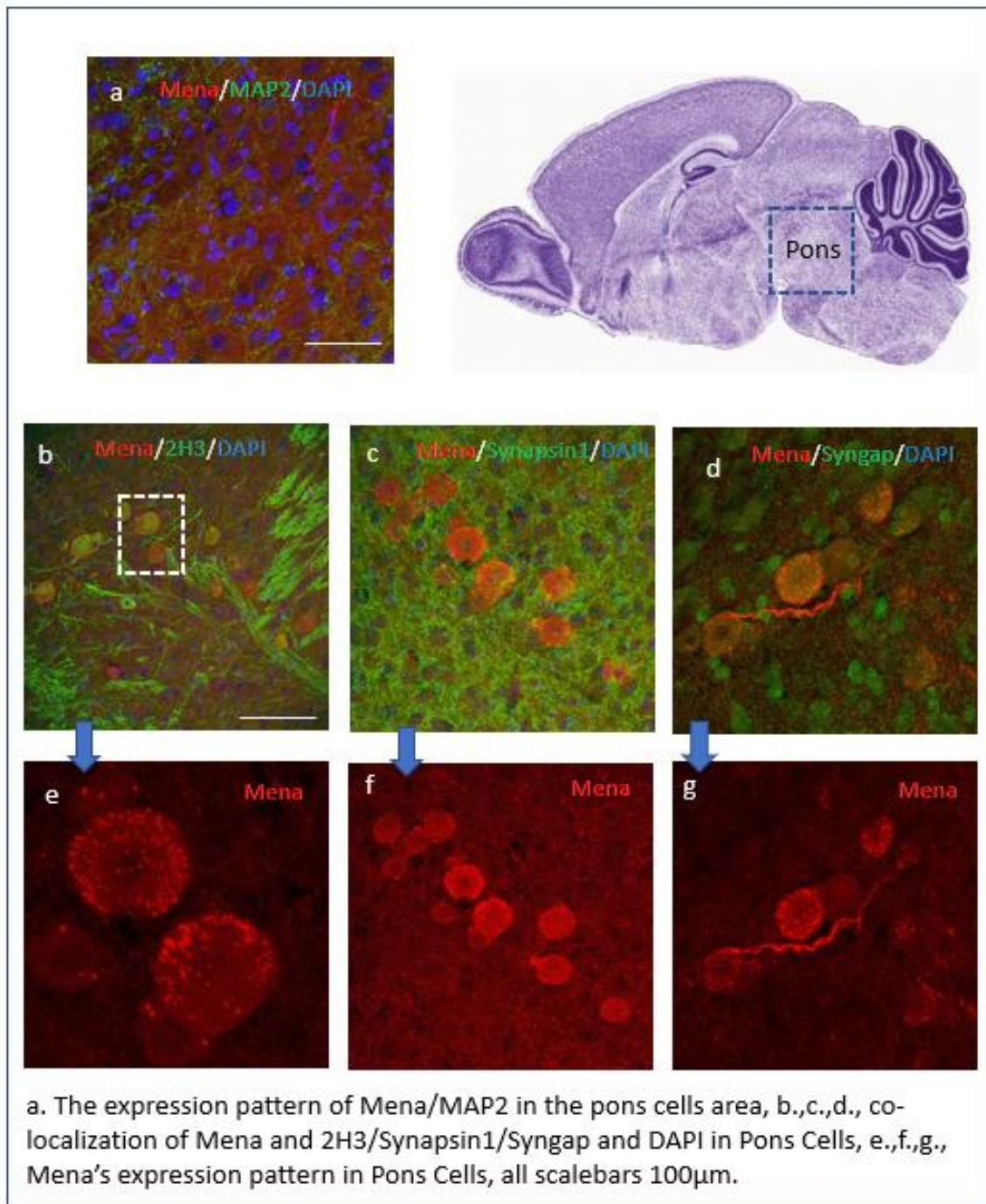


Image 20: Mena's localization in the P15 Pons cells area.

post-synaptic marker Syngap being observed (18c,d) in neurons, both in cell bodies and in axons. In the Corpus Callosum, a general co-localization with Mena and MAP2 was observed in the cell bodies, in a comparative pattern with the P8-10 timepoint. Similarly, the Olfactory bulb shows a strong Mena expression pattern, but no definitive synaptic co-localization (18f,g).

P15 Medulla, Hindbrain

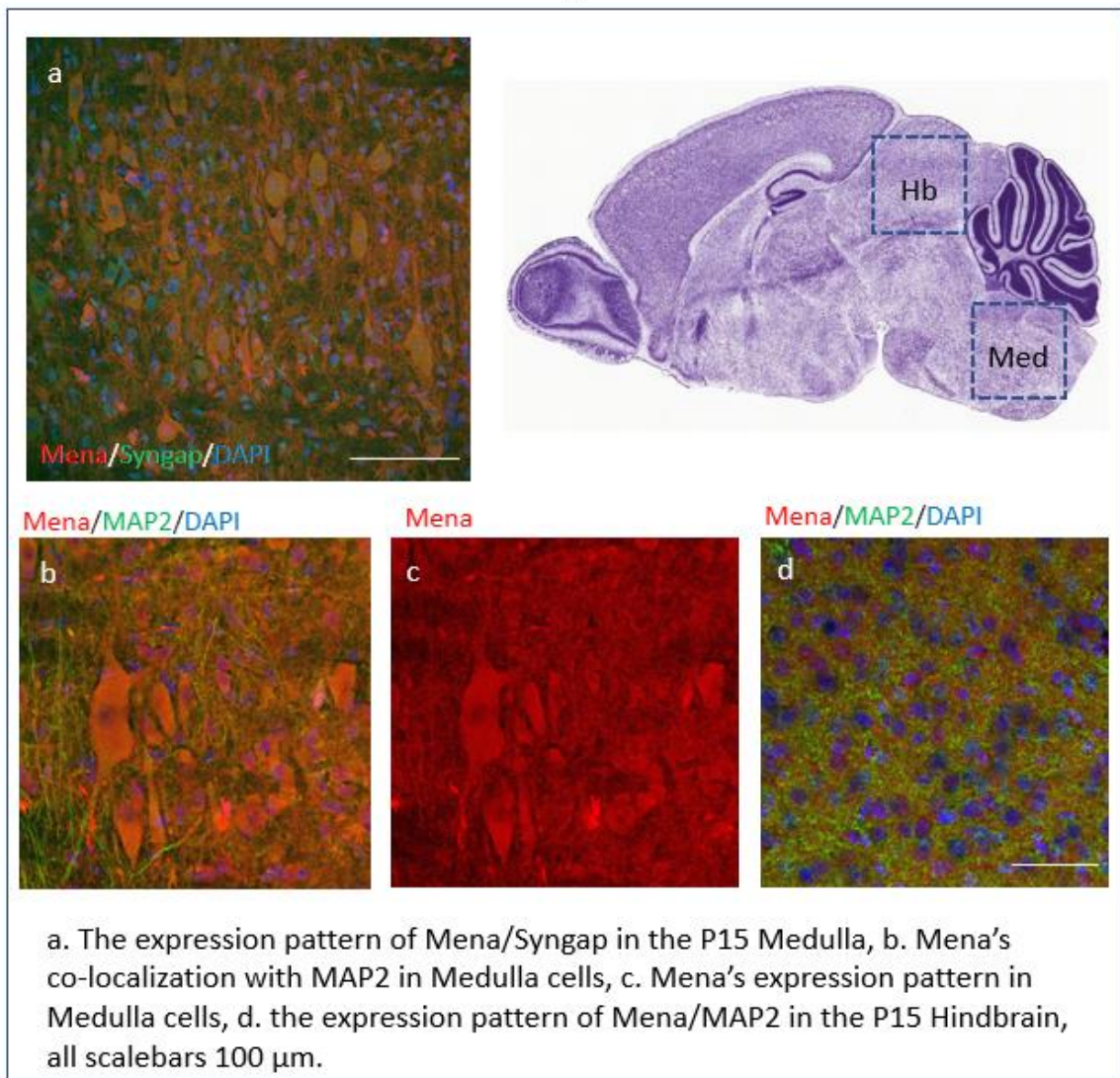


Image 21: Mena's localization in the P15 Medulla and Hindbrain.

In the Cerebellum, the similarities between P8-10 and P15 mice remain very evident. Purkinje cells retain their strong Mena immunoreactivity, and co-localization is consistently observed with Synapsin1, Syngap, and 2H3 (Image 19). In the case of 2H3, an interesting pattern is revealed, in which the signal of axonal marker 2H3 strongly encompasses the Mena-pronounced Purkinje cells. Mena's enhanced signal in concert with the enhanced axonal activity of Purkinje cells could be an interesting area of future research, especially given the implication of Purkinje cells in intellectual disorders in which Mena has also been implicated (Piochon et.al., 2014).

P15 Spinal Cord

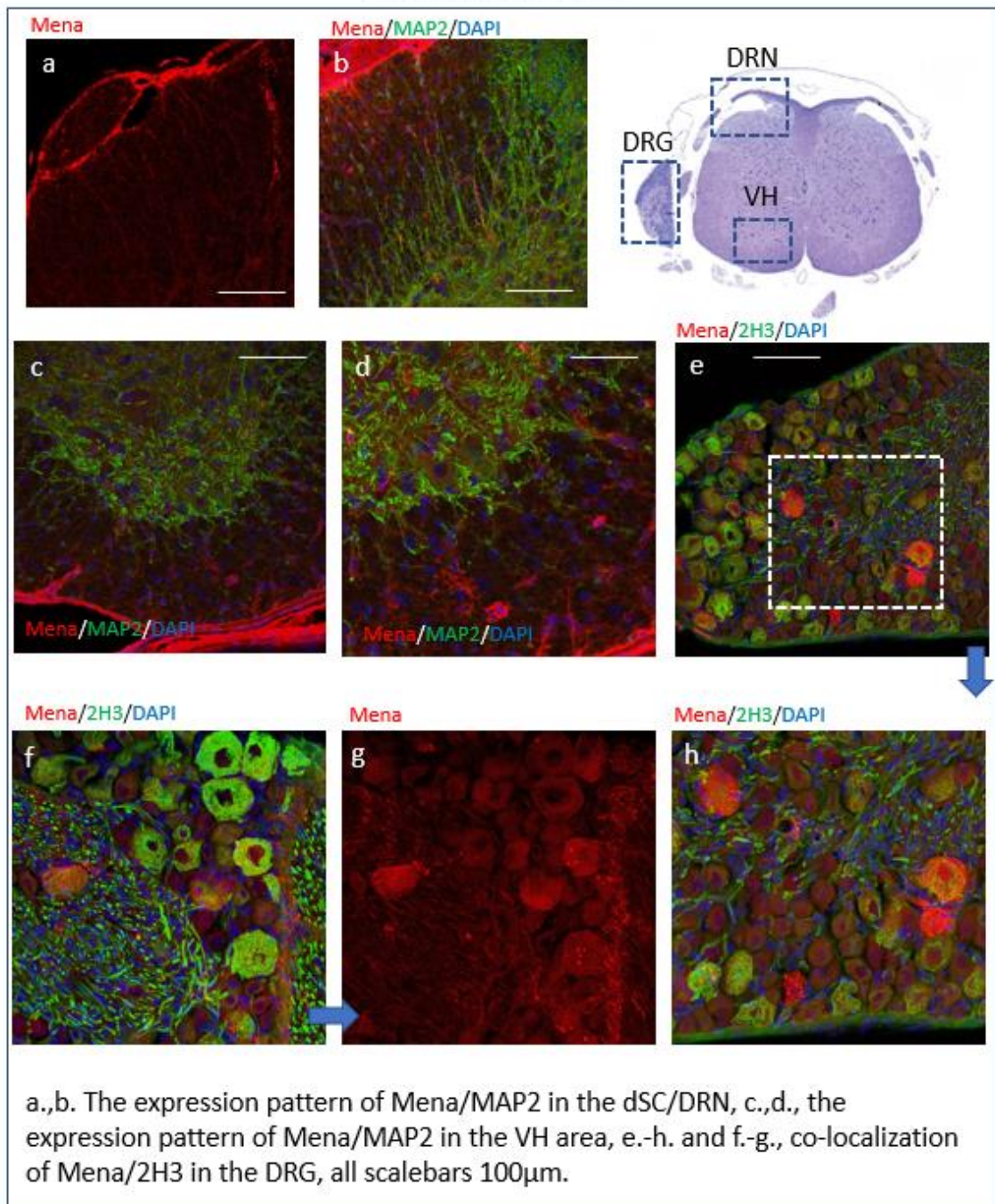


Image 22: Mena's localization in the P15 SC.

In the spinal cord, notable differences were once more not observed between the thoracic and lumbar areas. Mena's signal was again most pronounced in the DRGs area (22e,f,g,h). The dorsal root nerve (DRN) continued to show an increased Mena immunoreactivity pattern, with Mena staining axons (22a,b). The ventral horn (VH) area showed a slightly higher immunoreactivity, compared to the P8-10 timepoint, and cells could be observed with co-localization of Mena and MAP2 (22c,d).

C2. Biochemical analysis of Mena presence in synapses

Initially, the protocol (by Rubeis, Bagni et.al., 2011) for SN isolation was tested, in order to confirm the purification of the synaptoneurosome fragments. Western blot analysis was performed in isolated synaptoneurosome fragments (Image 23) and the protocol was found to indeed facilitate increased purification. More specifically, pre-synaptic and post-synaptic proteins such as synapsin1, synGAP and PSD95 were found to be increased in the isolated cortex synaptoneurosome fragments, and non-neuronal/non-synaptic proteins such as GFAP, NeuN and Tuj1 were found to be decreased. Mena as well as its interactors Hnrnpk and VASP were also isolated in the SNs, although in the case of Hnrnpk, it was isolated in a much smaller amount (Image 23).

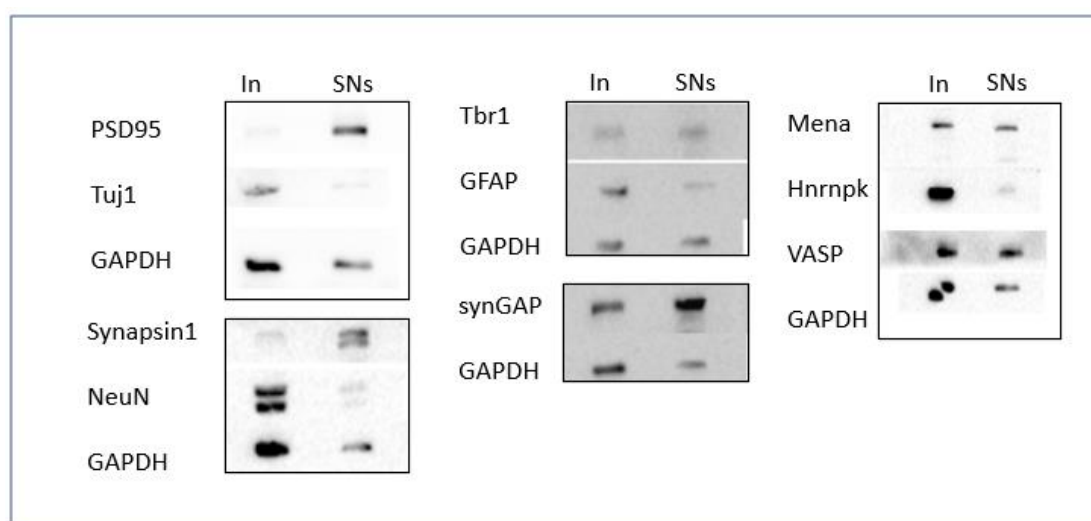


Image 23: Western blot analysis of P21 isolated SNs.

Given that these first findings were so encouraging as to the synaptoneurosome purification potency of this protocol, we proceeded to run a number of test co-immunoprecipitation experiments on the isolated synaptoneurosome fragments, in order to ensure the validity of future co-immunoprecipitation results.

As you can see in Image 24, Mena was found to be sufficiently enriched after the co-immunoprecipitation experiment, and the IgG control was found to be clear. Mena's interactor VASP was also found to be slightly enriched, and absent from the IgG control. This experiment was repeated two more times and its validity was confirmed with VASP and actin as interactors (Image 25) before we moved on to other proteins of interest.

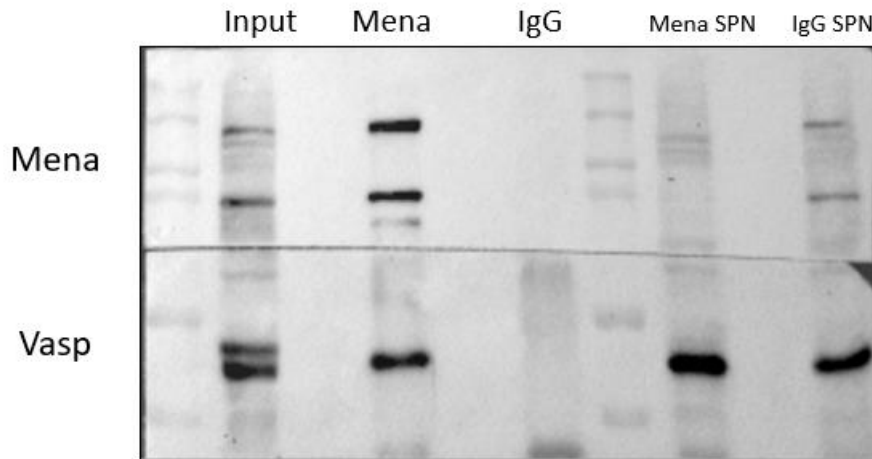


Image 24: 1-day co-IP protocol on P21 synaptoneurosomes, Abs tested: Mena, Vasp.

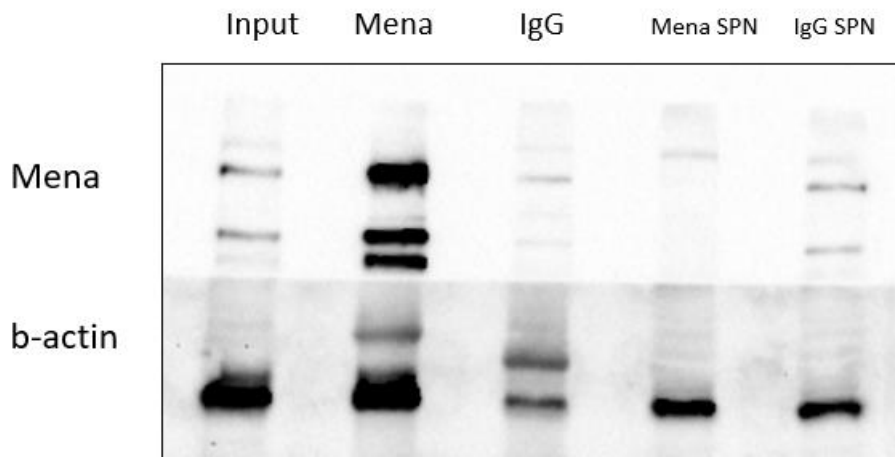


Image 25: 1-day co-IP protocol on P21 synaptoneurosomes, Abs tested: Mena, b-actin.

For the next series of experiments, a new input control was introduced. Lysate from the SNs was used as a second level of control, so that each protein's quantity in the synaptoneurosomes can be taken into account while interpreting the co-immunoprecipitation results.

Image 26 is a compilation of the most important co-immunoprecipitation results. Each protein was tested a minimum of 2 times, with the vast majority being tested at least 3. Mena and VASP, a very strong interactor, are used for comparison. Perhaps the most surprising and interesting result is that known interactors Hnrnpk and PCBP1 are not found to interact with Mena in synaptoneurosomes. EVL, another member of the Ena/VASP family, was found to interact with Mena and even presents an enhanced quantity. The other proteins of interest, EEF2 and SAFB, were also shown to interact with Mena in an enhanced manner.

P21 SNs co-IP

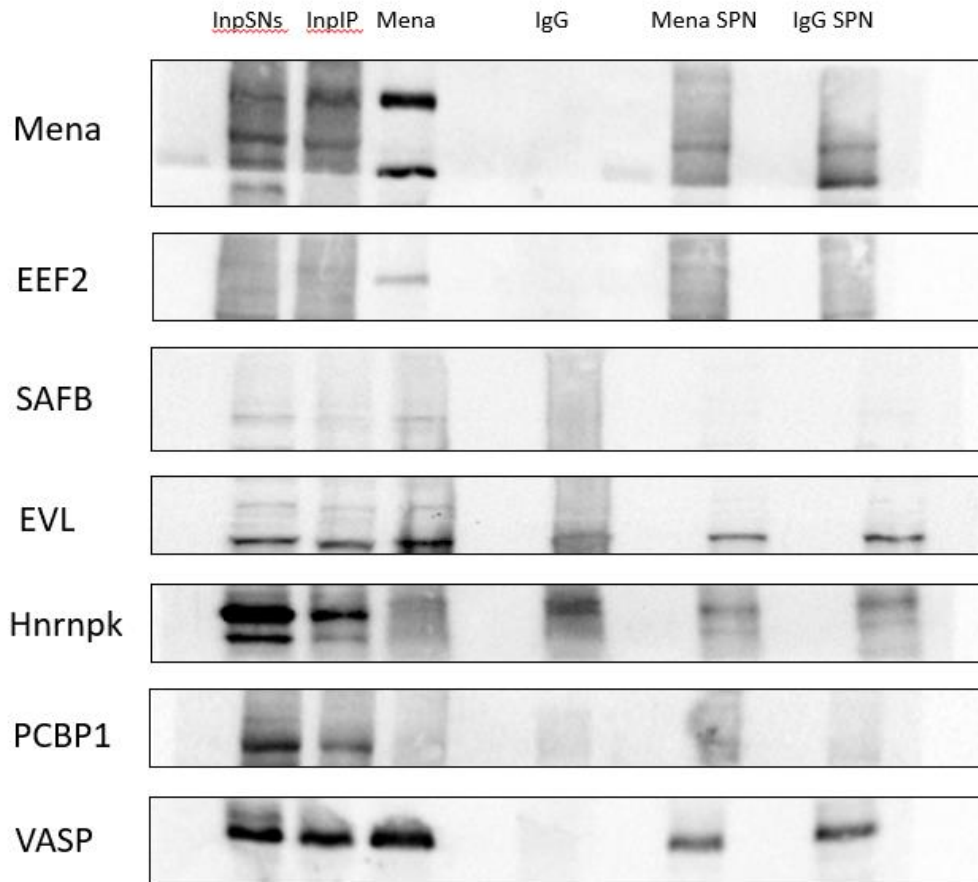


Image 26: Compilation of SNs co-IP results.

C.3 Concluding Remarks

During the immunofluorescence experiments, a number of similarities and differences were observed between the different timepoints, which could partially be explained due to the different neurodevelopmental processes taking place during these time periods. Some of the key differences were observed in the L2/3 and L5 layers of the cortex, the dentate gyrus of the hippocampus, and the hindbrain area. Perhaps most importantly for our series of experiments, in the cortex, P8-10 mice were found to not only have a more pronounced expression profile, but also showed more signs of Mena's synaptic localization. Taking into account the fact that the synaptoneurosome isolation protocol is mostly performed on P21 cortices, it would be advantageous for new timepoints to be added in the future, closer to the P8-10 timepoint, so as to have a more accurate representation of Mena's interaction profile throughout development. Such an adaptation of the protocol would most likely present its own challenges, perhaps most importantly due to the number of mice needed for each synaptoneurosome isolation

experiment. In isolating synaptoneuroosomes from such early timepoints, an even bigger number of mice would be needed. Different areas, such as the cerebellum, or other midbrain areas could be used for synaptoneurosome isolation instead, assuming that the protocol can be sufficiently modified.

In the isolated synaptoneuroosomes, we had perhaps the most surprising results. Hnrnpk and PCBP1, which have been found to form an RNP complex with Mena in neurons, were not found to interact with Mena in the synaptoneuroosomes. In the case of Hnrnpk, perhaps this is not as surprising: early experiments have shown that this factor exists in small quantities in the synaptoneuroosomes to begin with (Image 23) and this was further proven in the input controls of the SN co-IP experiments (Image 26). The reason for this discrepancy can only be theorized on, and presents a very interesting avenue for future research, in order to further validate these results and elucidate this key difference.

D – SUPPLEMENTARY MATERIAL

Bibliography

1. Biever, A. *et al.* (2019) ‘Local translation in neuronal processes’, *Current Opinion in Neurobiology*, 57, pp. 141–148. doi: 10.1016/j.conb.2019.02.008.
2. Holt, C. E., Martin, K. C. and Schuman, E. M. (2019) ‘Local translation in neurons: visualization and function’, *Nature Structural and Molecular Biology*. Nature Publishing Group, pp. 557–566. doi: 10.1038/s41594-019-0263-5.
3. Cioni JM, Koppers M, Holt CE. Molecular control of local translation in axon development and maintenance. *Curr Opin Neurobiol*. 2018 Aug;51:86-94. doi: 10.1016/j.conb.2018.02.025. Epub 2018 Mar 14. PMID: 29549711.
4. Bramham, C., Wells, D. Dendritic mRNA: transport, translation and function. *Nat Rev Neurosci* 8, 776–789 (2007).
5. Abekhoukh, S. and Bardoni, B. (2014) ‘CYFIP family proteins between autism and intellectual disability: Links with fragile X syndrome’, *Frontiers in Cellular Neuroscience*. Frontiers Research Foundation. doi: 10.3389/fncel.2014.00081.
6. Doyle M, Kiebler MA. Mechanisms of dendritic mRNA transport and its role in synaptic tagging. *EMBO J*. 2011 Aug 31;30(17):3540-52. doi: 10.1038/emboj.2011.278. PMID: 21878995; PMCID: PMC3181491.
7. Giuditta, A. *et al.* (2002) ‘Axonal and presynaptic protein synthesis: New insights into the biology of the neuron’, *Trends in Neurosciences*. Elsevier Limited, pp. 400–404. doi: 10.1016/S0166-2236(02)02188-4.
8. Sutton MA, Schuman EM (2006) Dendritic protein synthesis, synaptic plasticity, and memory. *Cell* 127: 49–58
9. Andreassi C, Riccio A (2009) To localize or not to localize: mRNA fate is in 3'UTR ends. *Trends Cell Biol* 19: 465–474.
10. Wang DO, Martin KC, Zukin RS (2010) Spatially restricting gene expression by local translation at synapses. *Trends Neurosci* 33: 173–182.
11. Cajigas IJ, Will T, Schuman EM (2010) Protein homeostasis and synaptic plasticity. *EMBO J* 29: 2746–2752.
12. Martin KC, Ephrussi A (2009) mRNA localization: gene expression in the spatial dimension. *Cell* 136: 719–730.
13. St Johnston D (2005) Moving messages: the intracellular localization of mRNAs. *Nat Rev Mol Cell Biol* 6: 363–375.
14. Maas, C. *et al.* (2012) ‘Formation of Golgi-derived active zone precursor vesicles’, *Journal of Neuroscience*. Society for Neuroscience, 32(32), pp. 11095–11108. doi: 10.1523/JNEUROSCI.0195-12.2012.
15. Kiebler, M. A. and Bassell, G. J. (2006) ‘Neuronal RNA Granules: Movers and Makers’, *Neuron*. Neuron, pp. 685–690. doi: 10.1016/j.neuron.2006.08.021.
16. Ross Buchan, J. (2014) ‘MRNP granules Assembly, function, and connections with disease’, *RNA Biology*. Landes Bioscience, pp. 1019–1030. doi: 10.4161/15476286.2014.972208.
17. Sasaki, Y. (2020) ‘Local translation in growth cones and presynapses, two axonal compartments for local neuronal functions’, *Biomolecules*. MDPI AG. doi: 10.3390/biom10050668.
18. Glock G., Heumueller M., Schuman EM (2017), mRNA transport and local translation in neurons, *current opinion in neurobiology*, 45, pp.169-177.
19. Kelleher RJ 3rd, Bear MF. The autistic neuron: troubled translation? *Cell*. 2008 Oct 31;135(3):401-6. doi: 10.1016/j.cell.2008.10.017. PMID: 18984149.
20. Liu, C. *et al.* (2017) ‘Loss of the golgin GM130 causes Golgi disruption, Purkinje neuron loss, and ataxia in mice’, *Proceedings of the National Academy of Sciences of the United States of America*. National Academy of Sciences, 114(2), pp. 346–351. doi: 10.1073/PNAS.1608576114/-/DCSUPPLEMENTAL.

21. Akins, M. R., Berk-Rauch, H. E. and Fallon, J. R. (2009) 'Presynaptic translation: Stepping out of the postsynaptic shadow', *Frontiers in Neural Circuits*. Front Neural Circuits. doi: 10.3389/neuro.04.017.2009.
22. Gurzu S, Ciortea D, Ember I, Jung I. The possible role of Mena protein and its splicing-derived variants in embryogenesis, carcinogenesis, and tumor invasion: a systematic review of the literature. *Biomed Res Int*. 2013;2013:365192. doi: 10.1155/2013/365192. Epub 2013 Jul 14. PMID: 23956979; PMCID: PMC3728509.
23. Gupton SL, Gertler FB, "Filopodia: the fingers that do the walking", 2007, *Sci. STKE* (400), re.5
24. Drees F, Gertler FB. Ena/VASP: proteins at the tip of the nervous system. *Curr Opin Neurobiol*. 2008 Feb;18(1):53-9. doi: 10.1016/j.conb.2008.05.007. Epub 2008 May 26. PMID: 18508258; PMCID: PMC2515615.
25. Gertler F, Condeelis J. Metastasis: tumor cells becoming MENAcing. *Trends Cell Biol*. 2011 Feb;21(2):81-90. doi: 10.1016/j.tcb.2010.10.001. Epub 2010 Nov 9. PMID: 21071226; PMCID: PMC3402095.
26. Menzies, A. S. *et al.* (2004) 'Mena and Vasodilator-Stimulated Phosphoprotein Are Required for Multiple Actin-Dependent Processes That Shape the Vertebrate Nervous System', *Journal of Neuroscience*. Society for Neuroscience, 24(37), pp. 8029–8038. doi: 10.1523/JNEUROSCI.1057-04.2004.
27. Lanier, L. M. *et al.* (1999) 'Mena Is Required for Neurulation and Commissure Formation', *Neuron*. Cell Press, 22(2), pp. 313–325. doi: 10.1016/S0896-6273(00)81092-2.
28. Kwiatkowski AV *et al.*, "Ena/VASP is required for neuritogenesis in the developing cortex", 2007, *Neuron* V. 56, issue 3, pp:441-455.
29. Dwivedy A *et al.*, 2007, "Ena/VASP function in retinal axons is required for terminal arborization but not pathway navigation", *Development* (2007) 134 (11):2137-2146.
30. N. Krumm, B.J. O'Roak, J. Shendure, E.E. Eichler "A de novo convergence of autism genetics and molecular neuroscience" *Trends Neurosci.*, 37 (2014), pp. 95-105.
31. B.J. O'Roak, L. Vives, W. Fu, J.D. Egerton, I.B. Stanaway, I.G. Phelps, G. Carvill, A. Kumar, C. Lee, K. Ankenman, *et al.* , "Multiplex targeted sequencing identifies recurrently mutated genes in autism spectrum disorders", *Science*, 338 (2012), pp. 1619-1622.
32. The Axon Initial Segment: An Updated Viewpoint, Christophe Leterrier, *Journal of Neuroscience* 28 February 2018, 38 (9) 2135-2145; DOI: 10.1523/JNEUROSCI.1922-17.2018
33. Bury, L. A. D. and Sabo, S. L. (2016) 'Building a Terminal: Mechanisms of Presynaptic Development in the CNS', *Neuroscientist*. SAGE Publications Inc., pp. 372–391. doi: 10.1177/1073858415596131.
34. Piochon, C., Kloth, A., Grasselli, G. *et al.* Cerebellar plasticity and motor learning deficits in a copy-number variation mouse model of autism. *Nat Commun* 5, 5586 (2014). <https://doi.org/10.1038/ncomms6586>
35. Kennedy, Heather & Jones, Charles & Caplazi, Patrick. (2013). Comparison of standard laminectomy with an optimized ejection method for the removal of spinal cords from rats and mice. *Journal of histotechnology*. 36. 86-91. 10.1179/014788813X13756994210382.

Abbreviations

P21 = 21 days of age

P22 = 22 days of age

P8-10 = 8 to 10 days of age

CNS = central nervous system

PNS = peripheral nervous system

NS = nervous system

RNP = ribonucleoprotein

SC = spinal cord

RT = room temperature

SNs = synaptoneuroosomes

PIs = protease inhibitors

SPN = supernatant

RBP = RNA-binding-protein

Cd = caudal

Ros = rostral

D = dorsal

V = ventral

Crx = cortex

PFC = prefrontal cortex

OB = olfactory bulb

Hb = hindbrain

Med = Medulla

Cer = Cerebellum

CC = corpus callosum

Th = Thalamus

HP = hippocampus

HF = hippocampal formation

DG = dentate gyrus

HTh = hypothalamus

L2/3 = layer 2/3 of the cortex

L5 = layer 5 of the cortex

DRG = dorsal root ganglion

DRN = dorsal root nerve

FB = forebrain

VH = ventral horn

Table of IF experiments

Title	Date of IF	Animal Name	Tissue	Dev. Day	Sex	Phenotype	Slide Nr	Ab 1	Ab 1 Dilution	Ab 2	Ab 2 Dilution	DAPI
IF0	29/09/21	AH3a_5	WB	P0	N/A	WT B6	1	NC		a-rb594	1/800 all	0,6/1000 all
							2	rb-Mena	1/250	a-rb594		
								ms-2H3	1/1000	a-ms488		
Title	Date of IF	Animal Name	Tissue	Dev. Day	Sex	Phenotype	Slide Nr	Ab 1	Ab 1 Dilution	Ab 2	Ab 2 Dilution	DAPI
IF1	19/10/21	AH5a_2	FB	P8-10	F	WT B6	10	ms-Mena	1/500	a-ms594	1/800 all	0,6/1000 all
								rb-MAP2	1/250	a-rb488		
							11	ms-Mena	1/500	a-ms594		
								rb-Synapsin1	1/500	a-rb488		
							12	rb-Mena	1/500	a-rb594		
								ms-2H3	1/1000	a-ms488		
							13	rb-Mena	1/500	a-rb594		
	ms-PSD95	1/250	a-ms488									
							14	NC top		a-ms594+a-rb488		
								NC bottom		a-ms488+a-rb594		
Title	Date of IF	Animal Name	Tissue	Dev. Day	Sex	Phenotype	Slide Nr	Ab 1	Ab 1 Dilution	Ab 2	Ab 2 Dilution	DAPI
IF2	9/11/2021	AH5a_2	Cer	P8-10	F	WT B6	7	NC top		a-ms594+a-rb488		0,6/1000 all
								NC bottom		a-ms488+a-rb594		
							8	ms-Mena	1/500	a-ms594		
								rb-MAP2	1/250	a-rb488	1/800 all	
							9	ms-Mena	1/500	a-ms594		
								rb-Synapsin1	1/500	a-rb488		
							10	rb-Mena	1/500	a-rb594		
								ms-2H3	1/1000	a-ms488		
								rb-Mena	1/500	a-rb594		
								ms-PSD95	1/250	a-ms488		
							(Test)	9/11/2021	AH5a_2	FB	P8-10	F
								T:rb-Vasp	1/500	a-rb488	1/1000	
								B:ms-Mena	1/400	a-ms594	1/2.000	
								B:rb-β3Tubulin	1/1000	a-rb488	1/1000	
Title	Date of IF	Animal Name	Tissue	Dev. Day	Sex	Phenotype	Slide Nr	Ab 1	Ab 1 Dilution	Ab 2	Ab 2 Dilution	DAPI
IF3FB	24/11/2021	AH5a_3	FB	P8-10	M	WT B6	1	ms-Mena	1/500	a-ms594	1/800 all	0,6/1000 all
								rb-MAP2	1/250	a-rb488		
							2	ms-Mena	1/500	a-ms594		
								rb-Synapsin1	1/500	a-rb488		
							3	rb-Mena	1/500	a-rb594		
	ms-2H3	1/1000	a-ms488									
							4	NC top		a-ms594+a-rb488		
								NC bottom		a-ms488+a-rb594		
(Test)							5	T:ms-Mena	1/500	a-ms594		
								T:rb-β3Tubulin	1/400	a-rb488		
								B: NC		a-ms594+a-rb488		
IF3Cer		AH5a_5	Cer	P8-10	M	WT B6	12	NC top		a-ms594+a-rb488		
								NC bottom		a-ms488+a-rb594		
							13	ms-Mena	1/500	a-ms594		
								rb-MAP2	1/250	a-rb488		
							14	ms-Mena	1/500	a-ms594		
								rb-Synapsin1	1/500	a-rb488		
							15	rb-Mena	1/500	a-rb594		
								ms-2H3	1/1000	a-ms488		

Title	Date of IF	Animal Name	Tissue	Dev. Day	Sex	Phenotype	Slide Nr	Ab 1	Ab 1 Dilution	Ab 2	Ab 2 Dilution	DAPI							
IF4	14/12/21	AH6b_2	SC w/bone	P15	N/A	WT B6	1	NC top		a-ms594+a-rb488		0,6/1000 all							
								NC bottom		a-ms488+a-rb594									
							2	ms-Mena	1/500	a-ms594									
								rb-MAP2	1/250	a-rb488	1/800 all								
							3	ms-Mena	1/500	a-ms594									
								rb-Synapsin1	1/500	a-rb488									
KO NC	MV4A9	FB	2 m.o.	F	Mena KO	13	NC		a-ms594+a-rb 488										
							ms-Mena	1/500	a-ms594										
							rb-Synapsin1	1/250	a-rb488										
						(Test)	AH7a_4	WBr	P22-25	N/A	WT B6	15	rb-Mena	1/500	a-rb594				
												ms-2H3	1/1000	a-ms488					
												NC		a-rb594+a-ms488					
IF5	12/1/2022	AH5a_3	SC w/bone	P8-10	N/A	WT B6	1	NC top		a-ms594+a-rb488		0,6/1000 all							
								NC bottom		a-ms488+a-rb594									
							2	ms-Mena	1/500	a-ms594									
								rb-MAP2	1/250	a-rb488	1/800 all								
							3	ms-Mena	1/500	a-ms594									
								rb-Synapsin1	1/500	a-rb488									
IF6	27/1/2022	AH6b_2	FB	P15	N/A	WT B6	2	NC top		a-ms594+a-rb488		0,6/1000 all							
								NC bottom		a-ms488+a-rb594									
							1	ms-Mena	1/500	a-ms594									
								rb-MAP2	1/250	a-rb488	1/800 a-ms								
							3	ms-Mena	1/500	a-ms594	1/1500 a-rb								
								rb-Synapsin1	1/500	a-rb488									
IF7FB	15/3/2022	AH6b_3	FB	P15	N/A	WT B6	5	rb-Mena	1/500	a-rb594									
								ms-2H3	1/1000	a-ms488									
							6	ms-Mena	1/500										
								rb-Syngap1	1/250	a-ms488									
							IF7Cer	15/03/22	AH6b_3	Cer	P15	N/A	WT B6	1	NC top		a-ms594+a-rb488		0,6/1000 all
															NC bottom		a-ms488+a-rb594		
2	ms-Mena	1/500	a-ms594																
	rb-MAP2	1/250	a-rb488	1/800 a-ms															
3	ms-Mena	1/500	a-ms594	1/1500 a-rb															
	rb-Synapsin1	1/500	a-rb488																
IF7Cer	15/03/22	AH6b_3	Cer	P15	N/A	WT B6	4	rb-Mena	1/500	a-rb594									
								ms-2H3	1/1000	a-ms488									
							5	ms-Mena	1/500										
								rb-Syngap1	1/250	a-ms488									

Title	Date of IF	Animal Name	Tissue	Dev. Day	Sex	Phenotype	Slide Nr	Ab 1	Ab 1 Dilution	Ab 2	Ab 2 Dilution	DAPI
IF8Cer	5/4/2022	AH6b_2	Cer	P15	N/A	WT B6	1	NC top		a-ms594+a-rb488		0,6/1000 all
								NC bottom		a-ms488+a-rb594		
							2	ms-Mena	1/500	a-ms594		
								rb-MAP2	1/250	a-rb488	1/800 a-ms	
							3	ms-Mena	1/500	a-ms594	1/1500 a-rb	
								rb-Synapsin1	1/500	a-rb488		
IF8SC	5/4/2022	AH5a_5	SC w/bone	P8-10	N/A	WT B6	4	rb-Mena	1/500	a-rb594		
								ms-2H3	1/1000	a-ms488		
							5	ms-Mena	1/500			
								rb-Syngap1	1/250	a-ms488		
							1	NC top		a-ms594+a-rb488		0,6/1000 all
								NC bottom		a-ms488+a-rb594		
2	ms-Mena	1/500	a-ms594									
	rb-MAP2	1/250	a-rb488	1/800 a-ms								
3	ms-Mena	1/500	a-ms594	1/1500 a-rb								
	rb-Synapsin1	1/500	a-rb488									
IF9	20/06/2022	AH6b_3	SC	P15	N/A	WT B6	4	rb-Mena	1/500	a-rb594		
								ms-2H3	1/1000	a-ms488		
							5	ms-Mena	1/500	a-ms 594		
								rb-Syngap1	1/250	a-rb488		
							1	NC top		a-ms594+a-rb488		0,6/1000 all
								NC bottom		a-ms488+a-rb594		
2	ms-Mena	1/500	a-ms594									
	rb-MAP2	1/250	a-rb488	1/800 a-ms								
3	ms-Mena	1/500	a-ms594	1/1500 a-rb								
	rb-Synapsin1	1/500	a-rb488									